

INFLUENCE OF ALPHA-TOCOPHEROL ON LIPID OXIDATION PATHWAYS

by

Zhehan Jiang

Submitted in partial fulfilment of the requirements

for the degree of Master of Science

at

Dalhousie University

Halifax, Nova Scotia

April 15th, 2020

© Copyright by Zhehan Jiang, 2020

TABLE OF CONTENTS

TABLE OF CONTENTS.....	ii
LIST OF TABLES.....	v
LIST OF FIGURES.....	vi
ABSTRACT.....	ix
LIST OF ABBREVIATIONS AND SYMBOLS USED	x
ACKNOWLEDGEMENTS	xiii
CHAPTER 1 INTRODUCTION	1
1.1 BACKGROUND.....	1
1.2 LIPID OXIDATION AND OXIDATION PRODUCTS.....	2
1.3 ANTIOXIDANTS	6
1.4 ANALYSIS METHODS.....	12
1.5 Objectives.....	15
CHAPTER 2 MATERIALS AND METHODS.....	16
2.1 EXPERIMENTAL DESIGN.....	16
2.2 SAMPLE PREPARATION	17

2.2.1	Transmethylation.....	17
2.2.2	Solid Phase Extraction (SPE) Conditions.....	18
2.2.3	TMS Derivatization.....	18
2.3	GAS CHROMATOGRAPHY-MASS SPECTROMETRY (GC-MS) AND GAS CHROMATOGRAPHY-FLAME IONIZATION DETECTION (GC-FID).....	19
2.3.1	Analysis of A Standard Mixture Using GC-MS.....	19
2.3.2	GC-MS Parameters	19
2.3.3	GC-FID Parameters.....	20
2.4	QUANTITATIVE ANALYSIS.....	21
2.4.1	Response Factors.....	21
2.4.2	Statistical Analysis.....	21
CHAPTER 3	RESULTS.....	23
3.1	IDENTIFICATION OF OXIDATION PRODUCTS IN OILS.....	23
3.1.1	Characteristic Electron Ionization (EI) Spectra of Oxidation Products	23
3.1.2	Identification of Oxidation Products by GC-MS	26
3.2	QUANTITATIVE ANALYSIS OF OXIDATION PRODUCTS IN OILS.....	35
3.3	MODELING OF OXIDATION RATE	39

CHAPTER 4	DISCUSSION.....	44
4.1.	IDENTIFICATION OF OXIDATION PRODUCTS	44
4.2.	QUANTIFICATION OF OXIDATION PRODUCTS	50
4.3	THE INFLUENCE OF ALPHA-TOCOPHEROL ON OXIDATION PATHWAYS	52
4.3.1	The Antioxidant and Prooxidant Capacity of α -Tocopherol	52
4.3.2	The Formation of Epoxides	56
4.3.3	The Formation of Aldehydes	58
CHAPTER 5	CONCLUSION.....	59
REFERENCES.....		61

LIST OF TABLES

Table 1	Oxidation plan for samples heated at 30 °C. ‘n’ indicates number of samples removed from the oven at that time point.....	17
Table 2	Identification of oxidation products in Polar Fraction 2 using spectra from both EI and CI modes, referring to the peaks labelled in Fig. 3.....	28
Table 3	Estimates of oxidation rates (k) and their confidence interval of groups treated with tocopherol at different concentrations derived from the exponential model fit to the data obtained. For an oxidation product, mean values with different superscripts are significantly different (pooled variance t-test; p<0.05).....	43

LIST OF FIGURES

Fig. 1. 1	Peroxide radicals attack double bonds, forming epoxides, and releasing alkoxy radicals (Giuffrida et al., 2004; Schaich, 2012).	5
Fig. 1. 2	There are two oxidation pathways leading to the formation of lipid alcohols. In one, lipid radicals are directly attacked by hydroxyl radicals; in the other, alkoxy radicals derived from peroxides abstract hydrogens from other lipids.	6
Fig. 1. 3	The hydrogen donated by BHA reacts with peroxide and alkyl radicals to generate phenolic radicals that are stabilized by resonance and can react further with other lipid or peroxy radicals.	8
Fig. 1. 4	Carnosol (a) and carnosic acid (b) are the major components of rosemary extracts and their phenolic structures can donate hydrogen atoms to lipid radicals.	10
Fig. 1. 5	Structures of tocopherols: (a) α -tocopherol ($R_1, R_2, R_3 = \text{methyl}$), (b) β -tocopherol ($R_1, R_3 = \text{methyl}$), (c) γ -tocopherol ($R_2, R_3 = \text{methyl}$), (d) δ -tocopherol ($R_3 = \text{methyl}$). * indicates the hydrogen atom donated to lipid radical in an antioxidation reaction.	12
Fig. 3. 1	The total ion chromatograms from (a) polar fraction 1 and (b) polar fraction 2 of standards. Peaks are labelled as follows: 1) indicates internal standard (19:0); 2) indicate 9,10-epoxyoctadecanoate methyl ester; 3) indicates 13-HODE; 4) show an unidentified tail coeluted with peak 3 and 5) a peak identified as trans 13-HODE.	24
Fig. 3. 2	Electron ionization cleavage of (a) linoleic acid, (b) 13-HODE, (c) 9-HODE, (d) 9,10-epoxy-12-octadecenoic acid methyl ester, (e) 12,13-epoxy-9-octadecenoic acid methyl ester, and (f) 9,10-12,13-diepoxyoctadecenoic acid methyl ester. The structure of methyl nonadecanoic acid (internal standard) which has 312 m/z (molecular ion) as a characteristic peak is not presented.	25
Fig. 3. 3	GC-MS total ion chromatograms of aldehydes, hydroxy FAME TMS derivatives and hydroxy-epoxy FAME TMS derivatives in Polar Fraction 2 derived from trilinolein oxidized at 30 °C for 5 days, with peak identities listed in Table 2. * indicates unidentified TMS derivatives with 73 m/z ion mass in mass spectrum, suggesting that they were hydroxy compounds. The MS filament was on from 20 min to 53.8 min.	26
Fig. 3. 4	Nonanoic acid, 9-oxo-, methyl ester	27

Fig. 3. 5 ^a EI mass spectrum of (a) tail of 13-HODE standard, (b) 13-HODE standard, (c) (d) tail of 9-HODE in sample and (e) 9-HODE in sample.....	29
Fig. 3. 6 ^b EI mass spectrum of (a) tail of 13-HODE standard, (b) 13-HODE standard, (c) (d) tail of 9-HODE in sample and (e) 9-HODE in sample.....	30
Fig. 3. 7 ^c EI mass spectrum of (a) tail of 13-HODE standard, (b) 13-HODE standard, (c) (d) tail of 9-HODE in sample and (e) 9-HODE in sample.....	31
Fig. 3. 8 Probable cleavage of (a) 9-HODE (b) 14-hydroxy octadecadienoic acid methyl ester, (c) 5-hydroxy octadecadienoic acid methyl ester and (d) two radicals with masses that match the ions peak in the spectra.	32
Fig. 3. 9 ^a Mass spectrum at EI mode (a) and PCI mode (b) of peak 9 in Fig. 1, suggesting that the compounds were co-eluting methyl 11-OTMS-9,10-epoxyoctadec-12-enoate and 11-OTMS-12,13-epoxyoctadec-9-enoate (both with molecular mass of 398). The m/z 285 ion arises from methyl 11-OTMS-12,13-epoxyoctadec-9-enoate and the 199 ion is derived from 11-OTMS-9,10-epoxyoctadec-12-enoate. Total ion chromatogram (c) and single ion chromatogram (d) of those compounds were also plotted.....	33
Fig. 3. 10 ^b Mass spectrum at EI mode (a) and PCI mode (b) of peak 9 in Fig. 1, suggesting that the compounds were co-eluting methyl 11-OTMS-9,10-epoxyoctadec-12-enoate and 11-OTMS-12,13-epoxyoctadec-9-enoate (both with molecular mass of 398). The m/z 285 ion arises from methyl 11-OTMS-12,13-epoxyoctadec-9-enoate and the 199 ion is derived from 11-OTMS-9,10-epoxyoctadec-12-enoate. Total ion chromatogram (c) and single ion chromatogram (d) of those compounds were also plotted.....	34
Fig. 3. 11 ^c Mass spectrum at EI mode (a) and PCI mode (b) of peak 9 in Fig. 1, suggesting that the compounds were co-eluting methyl 11-OTMS-9,10-epoxyoctadec-12-enoate and 11-OTMS-12,13-epoxyoctadec-9-enoate (both with molecular mass of 398). The m/z 285 ion arises from methyl 11-OTMS-12,13-epoxyoctadec-9-enoate and the 199 ion is derived from 11-OTMS-9,10-epoxyoctadec-12-enoate. Total ion chromatogram (c) and single ion chromatogram (d) of those compounds were also plotted.....	35
Fig. 3. 12 ^a Mean concentrations and standard deviations of (a) 13-HODE, (b) 9-HODE, (c) aldehyde and (d) epoxy-hydroxy-FAME in oxidized linoleic acid methyl ester at different time points quantified by GC-FID. At each sampling time, different letters indicate significantly different concentrations (ANOVA; n=3; p < 0.05).	37
Fig. 3. 13 ^b Mean concentrations and standard deviations of (a) 13-HODE, (b) 9-HODE, (c) aldehyde and (d) epoxy-hydroxy-FAME in oxidized linoleic acid methyl ester at different time points quantified by GC-FID. At each sampling time, different letters indicate significantly different concentrations (ANOVA; n=3; p < 0.05).	38

Fig. 3. 14 ^a	Oxidation rate model of 13-HODE and 9-HODE	40
Fig. 3. 15 ^b	Oxidation rate model of Aldehyde	41
Fig. 3. 16 ^c	Trendline fitted by natural logarithm of the initial concentration of (A) 13-HODE, (B) 9-HODE, (C) aldehydes and (D) epoxy-hydro-FAME in linoleic acid methyl ester during 15-day experimental cycle. Data are fitted with Equation 2.2 and corresponding parameters are found in Table 3. The samples treated with no tocopherol, 0.1% tocopherol and 2% tocopherol were labelled as (i), (ii) and (iii) respectively. The dotted lines show the confidence intervals of their oxidation rates (k in equation 2.1).	42
Fig. 4. 1	Two probable pathways can produce epoxy-hydroxy FAME from (a) hydroperoxides and (b) epoxides during oxidation.....	47
Fig. 4. 2	Hydroperoxides decompose following a mechanism that proceeds through hydroxy-epoxy structures to end with the formation of aldehydes (Raghavamenon et al., 2009).	48
Fig. 4. 3	Two products are derived from the decomposition of a peroxide radical. G indicates diacylglycerol backbone.	49
Fig. 4. 4	Mechanism of the prooxidant capacity of α -tocopherol, where L is lipid chain.	54

ABSTRACT

In this study, the focus was the qualitative and quantitative analysis of epoxides, hydroxides and aldehydes produced during oxidation of a single triacylglycerol, trilinolein, in the presence and absence of α -tocopherol, to better understand the diversity of products produced and the rates of their formation. Although α -tocopherol has a well-known antioxidant effect at low concentrations, it may also function as a prooxidant at high concentrations. To address this, α -tocopherol was added to trilinolein at two concentrations (0.1% and 2% by mass) and compared to a control sample without added tocopherol. All the samples were heated at 30 °C with aliquots removed for analysis every 3 days in a 15-day experimental cycle. Results clearly demonstrated the antioxidant capacity of α -tocopherol at 0.1%, with oxidation products present in lower concentrations and increasing more slowly than in the other treatments. Although earlier formation of hydroxides and aldehydes was obvious in samples treated by 2% α -tocopherol, the prooxidant capacity of α -tocopherol could not be statistically proven because of the high variation between replicates. The absence of epoxides and the presence of epoxy-hydroxy lipids suggested that the formation of hydroperoxides, accelerated by high concentrations of tocopherol, dominated over alternative oxidation pathways. Further, only one type of aldehyde was identified and quantified successfully and its concentration was much higher than the other products. Its structure suggested that the decomposition of hydroperoxides led to formation of hydroxides, epoxy-hydroxy lipids and finally aldehydes, in a step-by-step process. Hence, the formation of aldehydes reduced the concentrations of the other products, which might influence conclusions about tocopherol's prooxidant activity. Further investigation will be carried out by identifying and quantifying hydroperoxides to prove the alteration of the oxidation pathways in this study.

LIST OF ABBREVIATIONS AND SYMBOLS USED

ANOVA	Analysis of variance
AOCS	American Oil Chemists' Society
APCI	Atmospheric pressure chemical ionization
BHA	Butylated hydroxyanisole
BHT	Butylated hydroxytoluene
CI	Chemical ionization
°C	Degrees Celsius
DHA	Docosahexaenoic acid
EI	Electron ionization
EPA	Eicosapentaenoic acid
ESI	Electrospray ionization
FAME	Fatty acid methyl ester
GC-MS	Gas chromatography-mass spectrometry
GC-FID	Gas chromatography-flame ionization detector

13-HODE	Methyl 13-hydroxyoctadeca-9,11-dienoate
9-HODE	Methyl 9-hydroxyoctadeca-10,12-dienoate
HPLC	High performance liquid chromatography
LH	Unsaturated lipid
L•	Alkyl lipid radical
LO•	Alkoxy lipid radical
LOO•	Peroxy lipid radical
NIST	National Institute of Standards and Technology
NMR	Nuclear magnetic resonance
PG	Propyl gallate
PV	Peroxide value
<i>p</i> AV	<i>p</i> -Anisidine value
SIM	Single ion chromatogram
SPE	Solid phase extraction
TBHQ	<i>tert</i> -Butylhydroquinone
TIC	Total ion chromatogram

TMS	Trimethylsilyl
TSP	Thermo-spray ionization
α	Alpha
β	Beta
δ	Delta
γ	Gamma

ACKNOWLEDGEMENTS

I would like to express my deep appreciation to my supervisor, Dr. Sue Budge, and committee members, Dr. Gianfranco Mazzanti and Dr. Jenna Ritter, for their patient guidance, enthusiastic encouragement and valuable critiques. This research would not have been possible without their support and suggestions. I would also like to press my gratitude to the Marine Lipids Lab, Carrie Greene, Anna-Jean Reid, Christopher Barry, Rosemarie Hughes, Mike Cheng, Stephen Williams, Steven Duerksen, Laura Helenius and all the past students and co-workers, not only for their tremendous support during lab work, but also for their care and concern in daily life, what makes me have a feeling of home. Special thanks are owed to my co-workers and friends, Wei Xia and Liyun Ye. Thank you for your patient advice and guidance about doing research and solving difficulties. Lastly, to my parents, thank-you for your long-distance trust and support during the whole journey.

CHAPTER 1 INTRODUCTION

1.1 BACKGROUND

Lipids have been known as vital aspects of daily human nutrition for more than 60 years. They are deeply involved in the metabolism of the human body, as, for instance, they are major materials in cellular membrane synthesis, hormone production and even neural systems (McClements and Decker, 2008). As essential elements for human health, there are a variety of food products, such as vegetable oils, salad, cheese and frying foods, meeting our dietary needs for lipids. Fats and oils, which are the main form of food lipids, are also able to provide moisture and tenderization for breads. Perhaps most importantly, they act as high heat transfer agents in a range of cooking techniques, improving both the taste and appearance of foods (Mcgee, 2004).

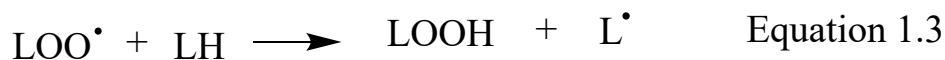
In foods, lipids can have a significant impact on the odor, color, texture and flavor, even when they are present at only minor concentrations (Frankel, 1984). Although food manufacturers developed oils extracted from vegetable sources such as soybean oil and peanuts oil, to meet the growing demand of customers, people soon noticed that vegetable oils rapidly turn rancid, producing unpleasant odors and deep colors after storage or heat processes, which raised concerns about lipid quality. Rancidity in fats and oils is due to the oxidation of unsaturated lipids. Hydrogenation processes have been conducted by the food industry for more than 30 years to remove polyunsaturated fats and therefore prevent oxidation and deterioration of lipids, until *trans*-fats were linked to cardiovascular toxicity in the last 15 years (Mozaffarian et al., 2006). Since then, lipid oxidation has once again become an important field of investigation.

Moreover, as people develop a deeper understanding of the composition of fat and its roles in human metabolism, their dietary preferences and structure also change. Almost 50 years ago, researchers observed that the Inuit population who consumed foods derived from marine species had lower incidence of coronary disease and diabetes mellitus, compared to populations in Denmark (Bang et al., 1971). Further research that followed found important evidence indicating that long-chain polyunsaturated fatty acids were the key ingredients responsible for those health benefits (Bang et al., 1976). Today, long-chain polyunsaturated fatty acids, especially eicosapentaenoic acid (EPA) and docosahexaenoic acid (DHA), are recognized as critical nutrients with important roles as anti-inflammatories and in improving cardiovascular health (Simopoulos, 1991). From non-fat or low-fat intake to consumption of polyunsaturated fatty acids as nutrients, research has shown that oils containing high concentrations of polyunsaturated fatty acids are susceptible to oxidation (Chan, 1987). In response to the increasing demand, more research about lipid oxidation and the means to prevent it, such as adding synthetic and natural antioxidants, are needed.

1.2 LIPID OXIDATION AND OXIDATION PRODUCTS

Lipid oxidation mechanisms have been studied for several decades and have been recognized as proceeding by a free radical chain reaction in three stages -- initiation, propagation and termination (Ingold, 1961; Schaich, 2012). Hydrogen abstraction creates free radicals, molecular oxygen adds to the radical, and further hydrogen abstractions establish and maintain the reaction (Schaich, 2005). Briefly, hydrogen abstraction, which is spontaneous and continual, produces alkyl radicals (Equation 1.1). Alkyl radicals are able to react with molecular oxygen, producing peroxide radicals (Equation 1.2). Peroxide radicals are quenched by abstracting

hydrogen atoms from nearby carbons atoms, forming hydroperoxides (Equation 1.3). In this classical autoxidation theory, hydroperoxides are considered as indicators of lipid oxidation in oil and they are recognized as primary oxidation products (Frankel, 1984).



Hydroperoxides are not the terminal products of lipid oxidation and they are likely to break down, producing an alkoxy radical which is highly reactive. Hydroxy compounds are formed from alkoxy radicals, since hydrogen abstraction is regarded as the preferred pathway in this reaction scheme. However, research has shown that there are other pathways, such as cyclization and β -scission competing with hydrogen abstraction (Schaich, 2005). Cyclization can produce epoxides or, with β -scission, reactive alkoxy radicals can result in cleavage of the aliphatic chain, producing an aldehyde and an alkyl radical (Frankel, 2005). Hydroxides, epoxides and aldehydes are recognized as secondary oxidation products; aldehydes have been considered as particularly important in assessing the extent of oxidation because they can be produced from both secondary products, hydroxides and epoxides, as well as from hydroperoxides, primary oxidation products. (Raghavamenon et al., 2009). Moreover, aldehydes are regarded as contributors to the off-flavor and toxicity of food products. They are highly biologically reactive, and can participate in various metabolic reactions, such as modifying lysine residues to form the oxidative low-density lipoprotein (Haberland et al., 1984; Jurgens and Esterbauer, 1986), which is likely to increase the

risks of atherosclerosis, cancer and heart disease (Valko et al., 2007). Therefore, aldehydes, long regarded as terminal oxidation products, have become recognized as important indicators of oil quality.

For polyunsaturated fatty acids, research has shown that products in addition to hydroperoxides, like epoxides and alcohols, form early in oxidation (Xie, 2015) (Xia and Budge, 2017); these oxygenated products have generally been recognized as secondary oxidation products, arising at the very end of the traditional lipid oxidation reaction mechanisms (Frankel, 1984). However, the mechanisms producing epoxides and alcohols require more attention. Different from hydroperoxide decomposition and rearrangement at the end of the classical oxidation reactions, several side pathways have also been put forward. As shown in Fig. 1.1, peroxide radicals attack double bonds in unsaturated fatty acids which break to form a cyclic oxygen structure and a peroxide which then loses an oxygen atom to generate an alkoxy radical (Giuffrida and Destailats, 2004). This reaction not only produces epoxides but also creates alkoxy radicals without proceeding through a hydroperoxide decomposition step which means it might potentially accelerate the oxidation process.

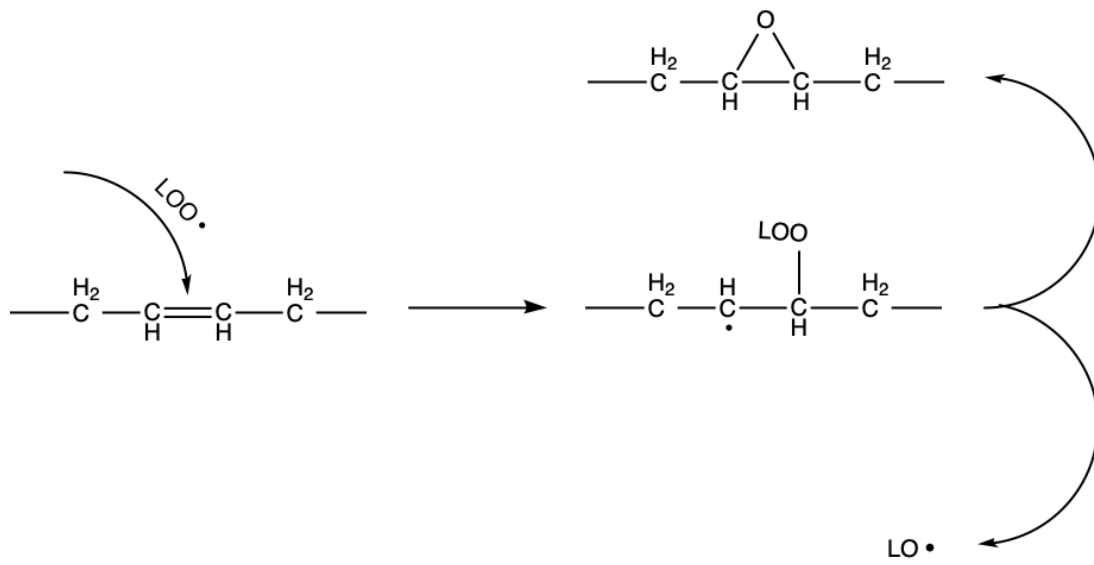


Fig. 1. 1 Peroxide radicals attack double bonds, forming epoxides, and releasing alkoxy radicals (Giuffrida et al., 2004; Schaich, 2012).

There are two main mechanisms that produce hydroxy lipids: 1) a lipid radical may be directly attacked by a hydroxyl radical (Repetto and Semprine 2012); and 2) an alkoxy radical may abstract a hydrogen from another lipid molecule (Fig. 1.2; McClements and Decker, 2008). These two pathways can also combine and create dihydroxy lipids from an alkoxy radical (Frankel, 1987). Schaich's work showed that hydrogen abstraction by alkoxy radicals is faster than by peroxy radicals, which means hydroxyl radicals in lipids might be a more relevant indicator of oxidation than hydroperoxides (Schaich, 2005). These pathways also show early formation of epoxides and alcohols in lipids oxidation. Moreover, instead of free fatty acids, these reactions generally involved intact lipids such as triacylglycerols and phospholipids (Weber, 1997). The oxidation products created from these are not volatile and are likely to undergo further reaction. Hence, the measurement of alternative lipids oxidation products, such

as epoxides and alcohols, is necessary for unsaturated fatty acids since the determination of hydroperoxides is not enough for the evaluation of the extent of oxidation.

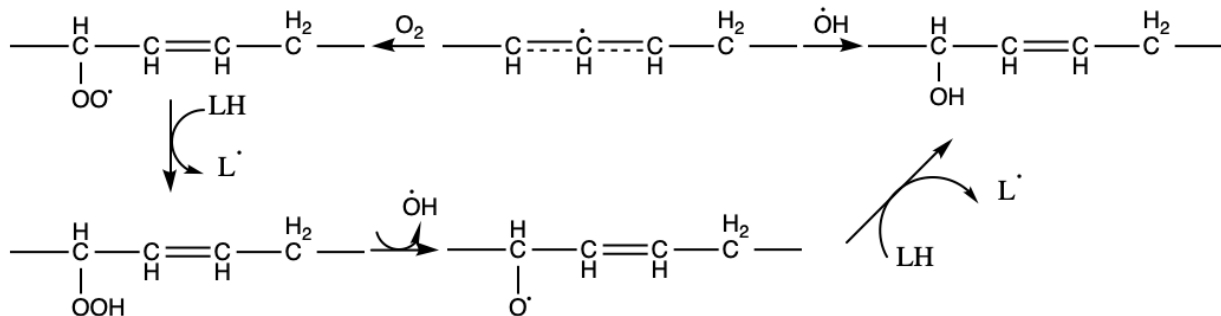


Fig. 1.2 There are two oxidation pathways leading to the formation of lipid alcohols. In one, lipid radicals are directly attacked by hydroxyl radicals; in the other, alkoxy radicals derived from peroxides abstract hydrogens from other lipids.

1.3 ANTIOXIDANTS

Preventing lipids from deterioration and prolonging the shelf life of lipid products has become one of the biggest challenges facing the food industry with the reduction in the use of the hydrogenation process. As the inhibition of lipid oxidation in oils is of vital importance, synthetic antioxidants, such as butylated hydroxyanisole (BHA), propyl gallate (PG) and *tert*-butylhydroquinone (TBHQ), have been widely used in commercial applications to prevent lipids from deteriorating. Frankel (1984) described the antioxidant mechanism of phenolic antioxidants (BHA, PG, TBHQ) as involving donation of hydrogen atoms to lipid radicals to produce relatively stable radicals that react very slowly with the lipid substrate. For instance, BHA can donate the hydrogen atom in its phenolic hydroxy group to a lipid radical or peroxide to prevent the formation of peroxy and alkoxy radicals (Fig. 1.3). The phenoxy radicals that are generated are stabilized by

resonance and are unlikely to react with lipid substrate (Frankel, 2005). The unpaired electron would be delocalized around the aromatic structure, allowing the phenoxy radical to generate more stable non-radical structures by reacting with peroxy radicals (Fig. 1.3). Thus, both the peroxy radicals and alkyl radicals on the lipid chain can be scavenged, thereby interfering with the initiation or the propagation of oxidation. In other words, phenolic antioxidants prevent lipid oxidation by interfering with both the formation and the decomposition of hydroperoxides. Frankel (1984) also alleged that phenolic compounds, such as these, at high concentrations and elevated temperatures would react with oxygen first and produce large amounts of phenolic radicals, which become prooxidants and chain-carriers, accelerating the lipid oxidation reaction. Literature has also suggested that all the phenolic antioxidants can behave as prooxidants; it depends on their concentration and the presence of transition metals (Villanueva, 2012). However, Fukumoto et al. (2000) analyzed multiple antioxidants by quantifying malonaldehyde in lipid samples and however, they found that BHT, BHA and α -tocopherol all behaved as antioxidants at concentrations between 0 to 4000 μ M (more than 20000 ppm); their antioxidant capacity also increased with increases in their concentration. This disagreement with previous work is likely because malonaldehyde was measured as the indicator of oxidation. That study suggests that secondary oxidation products, such as aldehydes, might not follow the prooxidant theory of α -tocopherol and that the lipid oxidation pathways may be altered in the presence of tocopherol.

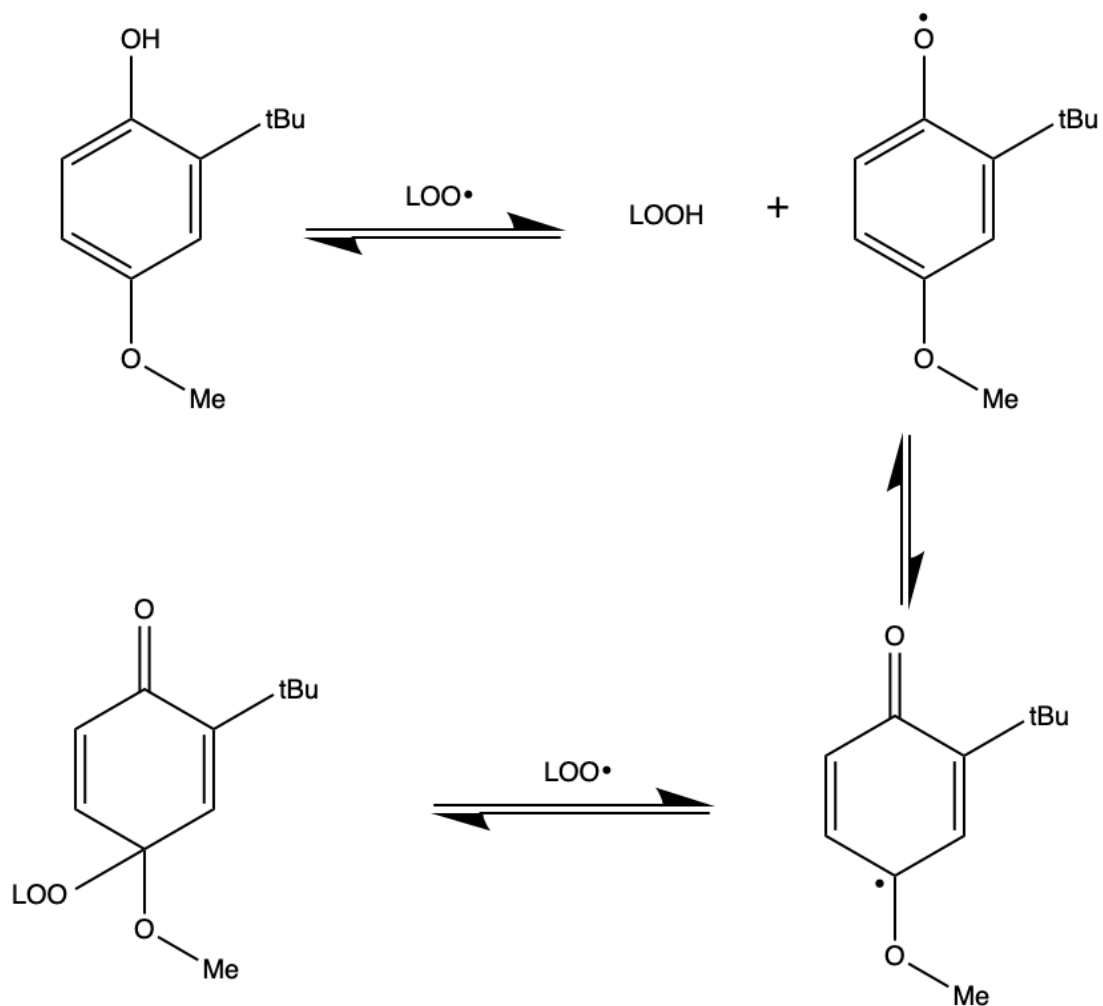


Fig. 1.3 The hydrogen donated by BHA reacts with peroxide and alkyl radicals to generate phenolic radicals that are stabilized by resonance and can react further with other lipid or peroxy radicals.

Although the anti- and pro-oxidation capacity and the reaction mechanisms of phenolic antioxidants have been studied for decades, there is still controversy about the mechanism associated with their prooxidant activity. Further, although the prooxidant theory of phenolic antioxidants is well-accepted, the optimum concentration and temperature for the best antioxidant

behavior have been less investigated, especially for natural antioxidants. This is particularly timely research, given the worldwide trend to avoid synthetic food additives and to replace them with natural antioxidants such as ascorbic acid, rosemary and tocopherol (Frankel, 1984).

Ascorbic acid is well-known as a complex multi-functional antioxidant, prooxidant and even a metal chelator (Barros et al., 2011). It is widely used in food applications for multiple purposes. In aqueous media, ascorbic acid has been shown to have antioxidant capacity at high concentrations (1 mM) and prooxidant capacity at low concentrations (0.1 mM) (Frankel, 2005). In oil media, although ascorbic acid is a more effective antioxidant, it is heavily influenced by the oxidation temperature, being less effective at 45 °C and more effective at 98 °C (Frankel, 2005). Because ascorbic acid is regarded as a secondary antioxidant which acts by scavenging oxygen (Gordon, 1990), its capacity also depends on the concentration of oxygen. Moreover, ascorbic acid and tocopherol have a well-known synergy, protecting oils from oxidation. Ascorbic acid can donate hydrogen atoms to tocopherol radicals, converting the radical back into the tocopherol parent (Frankel, 2005).

The antioxidant activity of rosemary extracts is mainly related to phenolic diterpene compounds, such as carnosol, carnosic acid (Fig. 1.4), rosmanol, epirosmanol and isorosmanol (Erkan et al., 2008; Richheimer et al., 1996). As the major antioxidant protection providers, carnosol and carnosic acid can effectively inhibit the formation of hydroperoxides in bulk vegetable oils and fish oil by donating hydrogen atoms and eliminating the radicals (Aruoma et al., 1992). Their antioxidant capacity is also influenced by the food matrix (Frankel, 2005). In oil-in-water emulsions, rosemary extracts will stay in the water phase reducing their protective ability; thus, they are most effective in bulk oils.

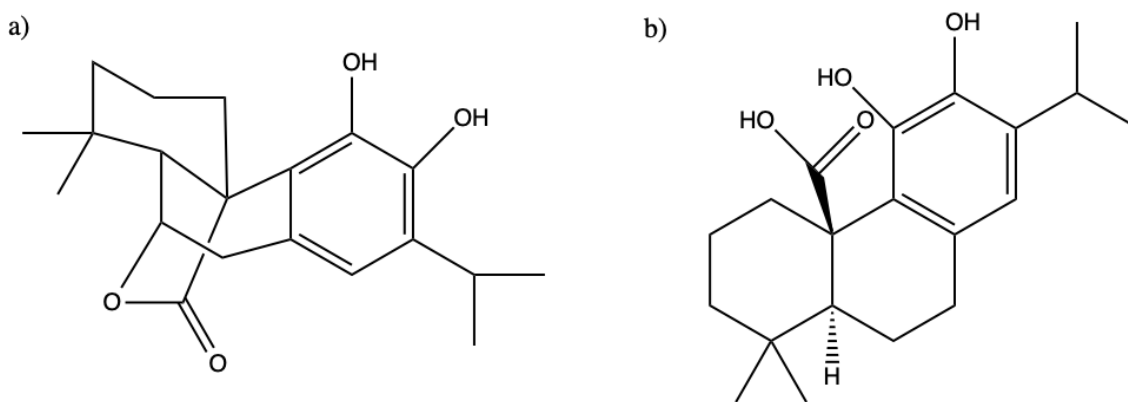


Fig. 1.4 Carnosol (a) and carnosic acid (b) are the major components of rosemary extracts and their phenolic structures can donate hydrogen atoms to lipid radicals.

In contrast to the broad knowledge of ascorbic acid and rosemary extracts, tocopherols are more of a mystery. Tocopherols are commonly found in most plants and fish (Pokorný, 2003). There are four different structures of tocopherols (Fig. 1.5) and they can donate hydrogen atoms to lipid radicals to prevent lipid chain from both propagation and decomposition, following the same mechanism as phenolic antioxidants. These four homologs are present in variable amounts in nature and are commonly added to different lipid products to increase their stability. A number of reports have clearly demonstrated the antioxidant capacity of α -tocopherol in methyl linoleate (Mäkinen and Hopia, 2000), rapeseed oil triacylglycerols (Lampi et al., 1999) and olive oil (Wagner and Elmadfa, 2000). However, these studies present conflicting conclusions about the antioxidant capacity of α -tocopherol, likely due to the use of different lipid substrates, tocopherol concentrations, analysis methods and temperatures.

Despite their wide-spread use, it has been known for ~30 years that tocopherols also possess prooxidant activity. Frankel (1984) reported that α -tocopherol had been shown to have a prooxidant capacity at high concentrations, as demonstrated by an increase in hydroperoxides at early stage of lipid oxidation; however, the mechanism for this is not well known. This phenomenon was also observed in some recent reports. For instance, using ^1H nuclear magnetic resonance (NMR), Martin-Rubio et al. (2018) found a similar result in that the concentrations of hydroperoxides, epoxides, ketones, hydroxy compounds and aldehydes increased at a more rapid rate in samples treated with 0.02% - 5% α -tocopherol (200 - 50000 ppm); they also found that oxidation was initiated earlier in the tocopherol-treated oil than in the control group. Hopia et al. (1996) also suggested that α -tocopherol at 40 mmol L⁻¹ (17240 ppm) accelerated the formation of hydroperoxides, as well as prevented hydroperoxides from decomposing. Moreover, Frankel (2005) also suggested that in polyunsaturated vegetable oils, tocopherols are normally known as poor antioxidants. For instance, crude soybean oil contains 1300 to 1500 ppm natural tocopherols and the removal of tocopherols actually increases the stability of soybean oil; the optimum concentration for soybean oil is between 400 and 600 ppm (Frankel et al., 1959a). Most importantly, the prooxidant mechanism of α -tocopherol has been rarely mentioned and remains unclear. European legislation allows the addition of α -tocopherol on the basis of the *quantum satis* principle (Commission Regulation 1129/2011) to refined vegetable oils, except refined olive oils, without an established limit. In other words, the negative effect of α -tocopherol is being neglected. Considering all of the above, a more comprehensive theory of the influence of α -tocopherol on the oxidative stability of lipid foods is clearly required.

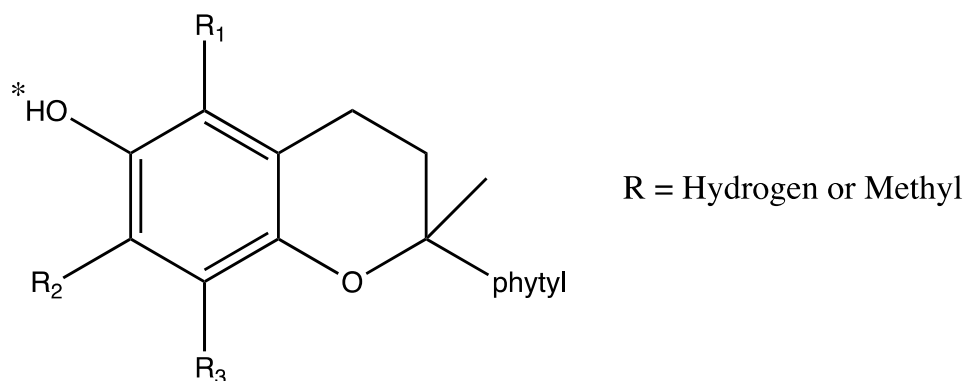


Fig. 1.5 Structures of tocopherols: (a) α -tocopherol ($R_1, R_2, R_3 = \text{methyl}$), (b) β -tocopherol ($R_1, R_3 = \text{methyl}$), (c) γ -tocopherol ($R_2, R_3 = \text{methyl}$), (d) δ -tocopherol ($R_3 = \text{methyl}$). * indicates the hydrogen atom donated to lipid radical in an antioxidation reaction.

1.4 ANALYSIS METHODS

The methods commonly used for determination of hydroperoxides and aldehydes are the widely applied titration method called the Peroxide Value (PV) and the spectrophotometric technique known as the *p*-Anisidine Value (PAV). They are the main methods used to judge the degree of oxidation (AOCS Method Cd 8-53; AOCS Method Cd 8b-90; AOCS Method Cd 18-90). In some analytical reports, conjugated dienes have also been measured using spectrophotometric techniques, while decomposition products of hydroperoxides including unsaturated aldehydes and volatiles have also been determined (Firestone, 2009). However, these methods do not provide any insight into the development of alternative oxidation products such as epoxides and hydroxides.

NMR Spectroscopy has been regarded as a powerful tool for analyzing fatty acid profiles (Knothe and Kenar, 2004). Previous NMR studies considered ^1H NMR as the major technique

applied to lipid oxidation analysis because of its relatively higher selectivity compared to the other commonly used nuclei such as ^{13}C and ^{31}P (Guill'en and Uriarte, 2012a). The most obvious advantage of NMR is the limited sample preparation required; techniques such as transmethylation and derivatization are easily avoided. NMR techniques have long been used to provide qualitative information about sample structures and composition but more recently have also been proven to be reliable for quantitative analysis (Mart'inez-Yusta et al., 2014). Additionally, NMR analysis can offer great time-savings, with different kinds of oxidation products determined in a single run, simply by dissolving samples in deuterated solvent. However, for polyunsaturated fatty acids, intact structure information is not available when NMR methods are applied. For instance, the position of double bonds remains unknown when the oxidation products are determined (Goicoechea and Guill'en, 2010). Moreover, compared to other analytical techniques such as gas chromatography (GC), NMR has relatively low sensitivity (Xia and Budge, 2017).

While high performance liquid chromatography (HPLC) has been used to separate oxidized fatty acids for decades (G'erard et al., 1992), identification of intact triacylglycerols has been regarded as the most valuable function of HPLC. However, the large number of possible structures of triacylglycerols combined with different esterified fatty acids make the identification challenging (Buchgraber et al., 2004). Hence, HPLC is typically coupled with mass spectrometry (MS) as an effective identification technique for analyzing structures in vegetable oils, lard and plasma samples (Marai et al., 1983). The MS ionization techniques which have been applied to HPLC are electrospray ionization (ESI) and atmospheric pressure chemical ionization (APCI) for identification of intact triacylglycerols, and thermo-spray ionization (TSP) for analysis of fatty acids or fatty acid methyl esters. For example, Gr'üneis et al. (2019) developed a method to identify the hydroperoxidized and epoxidized triacylglycerols in canola oil and margarine, which were

thermo-oxidized at 25 °C, 80 °C and 180 °C for 15, 30, 45, 60 minutes, using LC-ESI successfully. However, MS techniques applied to HPLC are all soft ionization techniques, leading to molecular ions and diacylglycerol fragments without fragments produced by hydrocarbon chain cleavage. In other words, although the oxidation products can be identified by analyzing molecular ions and diacylglycerol ions as in Grüneis et al. (2019), the position of hydroperoxyl, epoxy and even double bonds in the lipid chain cannot be assured.

Gas chromatography (GC) has been well-known as an effective method for analyzing small volatile compounds that form from β -scission during lipid oxidation. Common GC applications, such as GC-MS and GC-flame ionization detection (GC-FID), are effective methods for identification and quantification of oxidation products. For GC-MS, in contrast to LC-MS, among the ionization techniques that have been applied to GC, electron ionization (EI) has been discussed as the major method in identifying different structures by their distinct fragmentations produced from hydrocarbon cleavage; chemical ionization (CI) can be used as a supplemental method for identification of the mass of the molecular ion. For instance, with EI fragmentation, the location of a hydroxyl group in a fatty acid methyl ester can be determined from the ion masses of fragments produced by cleavages occurring on each side of the functional group (Weihrauch and others, 1974; Wilson and others 1997). Although GC methods cannot analyze compounds with high polarity, trimethylsilyl (TMS) derivatives have been widely applied to eliminate the polarity problem (Poole, 2013). For quantification, GC-FID has shown excellent selectivity for alternative oxidation products, but the identification of major oxidation products of lipids can be affected by coelution problems (Xia and Budge, 2017). To avoid co-elution of epoxides and hydroxides, Xia and Budge (2018) optimized a solid phase extraction (SPE) method for separating epoxides, hydroxides and non-polar FAME. In summary, although GC techniques require a time-consuming sample

preparation process, they are useful tools for qualitative and quantitative analysis of alternative oxidation products with appropriate pretreatment, including transmethylation, SPE and TMS derivatives (Marmesat et al., 2008).

1.5 Objectives

Bearing in mind all of the above, it is important to evaluate the effect of α -tocopherol on lipid oxidation pathways and the mechanism of its prooxidant capacity as accurately and completely as possible. In this research, the overall objective was to obtain a better understanding of anti- and pro-oxidation capacity and the associated mechanisms of α -tocopherol. To do this, a single type of triacylglycerol, trilinolein (18:2), was adopted as the lipid substrate and treated with 0.1% (1000 ppm) and 2% (20000 ppm) by weight α -tocopherol. Limited oxidation products are expected with the adoption of trilinolein, an approach rarely used in previous literature. By using a single TAG, the types of oxidation products can be reduced and the mechanism of lipid oxidation will be more obvious since the oxidation products can only be derived from 18:2 fatty acid. In addition, the effect of tocopherol naturally present in vegetable oils is thus eliminated. Since polyunsaturated fatty acid supplements are likely to be stored at room temperature, the temperature of thermal oxidation in this research was set at 30 °C, slightly above room temperature. Specifically, this work tests three hypotheses: 1) that low concentrations of tocopherol will have an anti-oxidant effect, in comparison to high concentrations; 2) that the secondary oxidation products will be produced following different oxidation pathways in the presence of tocopherol; and 3) the concentration of lipid alcohols will be higher with high concentrations of tocopherol due to the donation of hydrogen atoms.

CHAPTER 2 MATERIALS AND METHODS

2.1 EXPERIMENTAL DESIGN

Pure trilinolein (C18:2) (Sigma-Aldrich Inc.) was divided into 3 groups. Group 1 was the control, while group 2 and group 3 contained tocopherol at concentrations of 1.0 mg g⁻¹ and 20.0 mg g⁻¹ respectively. Groups I, II and III were sampled at five time points in triplicate. An additional initial time point for samples in Group I and II was also included without a replicate to eliminate the effect of products existing in trilinolein samples. Samples from Group III were not tested on day 1 because they are the same samples as those in Group II before the thermal oxidation process. Alpha-tocopherol (Sigma-Aldrich Inc.) was dissolved in hexane, preparing 60.0 mg L⁻¹ and 1200.0 mg L⁻¹ solutions. To create 1.0 mg g⁻¹ samples, 5.0 mL of the 60.0 mg L⁻¹ solution were added into empty test tubes that would become group II; 5.0 mL of the 1200.0 mg L⁻¹ solution were added into other test tubes to form the third group (at 20 mg g⁻¹). The same volume of hexane was also added to test tubes forming Group I so that the experimental control was treated in the same manner as the test samples. Hexane in test tubes in all three groups was then evaporated to dryness and 300 mg trilinolein was added to each. All samples were transferred to 4 mL open vials with approximately 3 mL of headspace and placed in a 30 °C oven with circulating air but without forced convection. All the vials remained open and three replicates were removed from each group following the oxidation plan (Table 1). After removal from the oven, the vials were purged with nitrogen, capped, and stored in the freezer at -30°C for several days until prepared for analysis.

Table 1 Oxidation plan for samples heated at 30 °C. ‘n’ indicates number of samples removed from the oven at that time point.

Oxidation time (days)	Group I (Control) n	Group II (0.1% tocopherol) n	Group III (2% tocopherol) n
0	1	1	0
2	3	3	3
5	3	3	3
7	3	3	3
10	3	3	3
15	3	3	3

2.2 SAMPLE PREPARATION

2.2.1 Transmethylation

Firstly, methanol was poured through a funnel with filter paper containing a bed of 10.0 g of anhydrous sodium sulfate to remove traces of water. Then 10 mL of 0.5 M sodium methoxide was diluted in 15 mL dry methanol (total volume 25 mL) to make a 0.2 M solution.

Secondly, each 100 mg trilinolein sample derived from 300 mg sample was placed in a 10 mL test tube to which were added 1 mL of *tert*-butyl methyl ether and 1 mL of 0.2 M sodium methoxide in methanol. The test tubes were shaken for 1 min and left to sit for 2 min. Then 0.1 mL of 0.5 M sulfuric acid in water was added, followed by addition of 3 mL of water. After

vigorous shaking and centrifugation, the top organic layer containing FAME was collected in a graduated test tube, and the solvent was evaporated under nitrogen.

2.2.2 Solid Phase Extraction (SPE) Conditions (Xia and Budge, 2018)

The FAME created from each trilinolein sample (~100 mg) were dissolved in 0.5 mL 98:2 (hexane:ethyl ether) and transferred to a solid phase extraction (SPE) column which was fixed to a glass chamber with 20 ports and fitted with a vacuum pump. The test tube was washed with 0.5 mL 98:2 (hexane:diethyl ether) solution, and the rinse was added to the SPE column. A gentle vacuum was applied to the columns with a three-step elution scheme:

a) Addition of 15 mL 98:2 (hexane:diethyl ether) to SPE column to elute the nonpolar fraction containing most of the linoleic acid methyl ester (C18:2).

b) Addition of 15 mL 90:10 (hexane:diethyl ether) to SPE column to elute polar fraction 1 containing epoxy FAME and traces of C18:2.

c) Addition of 30 mL diethyl ether to SPE column to elute polar fraction 2 containing hydroxyl FAME.

2.2.3 TMS Derivatization

Polar fractions 1 and 2 collected in section 2.2 were evaporated to dryness under nitrogen, mixed with 100 μ L N, O-bistrifluoroacetamide (BSTFA) and 100 μ L pyridine, and left to sit for

30 min at room temperature. After the reaction was complete, the sample was evaporated to dryness again and then dissolved in 200 μL hexane for GC analysis. Methyl nonadecanoate (19:0; 300 μL of 0.032 mg mL^{-1} solution) was added to both polar fractions (48 $\mu\text{g mL}^{-1}$) as an internal standard.

2.3 GAS CHROMATOGRAPHY-MASS SPECTROMETRY (GC-MS) AND GAS CHROMATOGRAPHY-FLAME IONIZATION DETECTION (GC-FID)

2.3.1 Analysis of a Standard Mixture Using GC-MS

A mixture of commercially available linoleic acid, and (S)-13-hydroxyoctadeca-9,11-dienoic acid (13-HODE) methyl ester (> 98%), and 9,10-epoxyoctadecanoate methyl ester synthesized as described in Xia and Budge (2018) was analyzed using GC-MS. The mixture was carried through the transmethylation, SPE and TMS derivatization procedure; internal standard (C19:0) was then added and the mixture analyzed using GC-MS. The retention time of each standard in the chromatograms was recorded.

2.3.2 GC-MS Parameters

A Trace 1310 gas chromatograph coupled with an ISQ7000 single quadrupole mass spectrometer was used to identify epoxy and hydroxy FAME. The samples were analyzed using a Rtx-2330 capillary column (90% biscyanopropyl/10% phenylcyanopropyl polysiloxane, 105 m \times 0.25 mm i.d., 0.2 μm). All polar fractions were introduced by a Thermo Fisher Scientific AIAS-1310 autosampler with a PTV injector at 250 $^{\circ}\text{C}$ in splitless mode and an injection volume of 1 μL . The temperature program started at 69 $^{\circ}\text{C}$ and was held for 2 min, increased to 174 $^{\circ}\text{C}$ at 15 $^{\circ}\text{C min}^{-1}$ and was held for 10 min, increased to 250 $^{\circ}\text{C}$ at 20 $^{\circ}\text{C min}^{-1}$ and was held for 31 min with

a total time of 53.8 min. The carrier gas was helium with constant flow at 1.2 ml min⁻¹. The MS detector was in a full scan electron ionization (EI) mode with the ion source and transfer line kept at 200 °C and 245 °C respectively, using an ionization potential of 70 eV with a mass scan range of m/z 60-600. For positive chemical ionization (PCI) analysis, methane was used as reagent gas at 1.5 mL min⁻¹. The other parameters remained the same as in EI mode.

In an attempt to improve resolution of co-eluting peaks, the samples were also analyzed using a DB-23 column ((50%-cyanopropyl)-methylpolysiloxane, 30m × 0.25 mm, 0.25 µm). The temperature program started at 50 °C and was held for 2 min, increased to 165 °C at 15 °C min⁻¹ and was held for 15 min, increased to 205 °C at 10 °C min⁻¹ and was held for 10 min, increased to 230 °C at 10 °C min⁻¹ and was held for 10 min with a total time of 51.17 min. The carrier gas was helium with constant flow at 1.2 ml min⁻¹. The other parameters remained the same as applied with the Rtx-2330 column.

2.3.3 GC-FID Parameters

After the analysis using GC-MS, GC-FID (Scion 436-GC, Bruker) was used with the same Rtx-2330 capillary column as above to quantify all the oxidation products. The samples were introduced by a Bruker CP-8400 autosampler with an injection volume of 1 µL. The GC parameters remained the same as applied in GCMS. The FID detector was set at 270 °C, with argon (make-up gas), hydrogen and air flow rates at 50, 30, 300 mL min⁻¹.

2.4 QUANTITATIVE ANALYSIS

2.4.1 Response Factors

Optimization of GC parameters and SPE recovery tests were previously carried out by Xia and Budge (2018). Methyl nonadecanoate (19:0) was used as the internal standard for GC-FID quantifications. Since trilinolein was used as the sample, the oxidation products expected were hydroxy-18:2, epoxy-18:1 and epoxy-18:0. Response factors were obtained for the hydroxy and epoxy compounds using 13-HODE methyl ester and 9,10-epoxyoctadecanoate methyl ester, respectively; 9,10-epoxyoctadecanoate methyl ester was synthesized as described in Xia and Budge (2018). Calibration curves were established by plotting the area ratio of analyte:internal standard versus the concentration of analyte. The working range was 5-60 $\mu\text{g ml}^{-1}$, with the internal standard at 48 $\mu\text{g ml}^{-1}$.

2.4.2 Statistical Analysis

SPSS[®] (IBM Software, Inc., USA) was used to perform an analysis of variance (ANOVA) to determine the influence of α -tocopherol at two concentrations on trilinolein samples. The α -level was set to 0.05.

For each oxidation product, there was a nonlinear relationship between concentration and time during the 15-day experimental cycle. To model that relationship, the following equation was used (SPSS, IBM Software, Inc., USA):

$$Y_f(d) = C_i * \exp^{kd} \quad 2.1$$

where $Y_f(d)$ is the concentration on a given day, C_i is the concentration on the first day, k is the rate of oxidation (reaction constant), and d is the number of days of oxidation.

For a more obvious comparison of the oxidation rates (k) among the three groups, the exponential curve was converted into a linear regression curve by taking the natural logarithm of both sides of equation 2.1, yielding equation 2.2.

$$\ln[Y_f(d)] = \ln(C_i) + kd \quad 2.2$$

Pooled variance t-tests were applied to the oxidation rates (k) derived from the linear regression models (SPSS, IBM Software, Inc., USA) with α set at 0.05 indicating significant differences.

CHAPTER 3 RESULTS

3.1 IDENTIFICATION OF OXIDATION PRODUCTS IN OILS

3.1.1 Characteristic Electron Ionization (EI) Spectra of Oxidation Products

Polar fraction 1 of the standard mixture showed two peaks: the internal standard (19:0) and 9,10-epoxyoctadecanoate methyl ester. Polar fraction 2 showed the internal standard, *cis*-13-HODE, a co-eluting shoulder and a small amount of *trans*-13-HODE. (Fig. 3.1.)

Based on structure, characteristic cleavage patterns of the anticipated oxidation products can be predicted (Xia and Budge, 2017) (Fig. 3.2.). The mass spectra of oxidized samples were evaluated for these cleavage patterns.

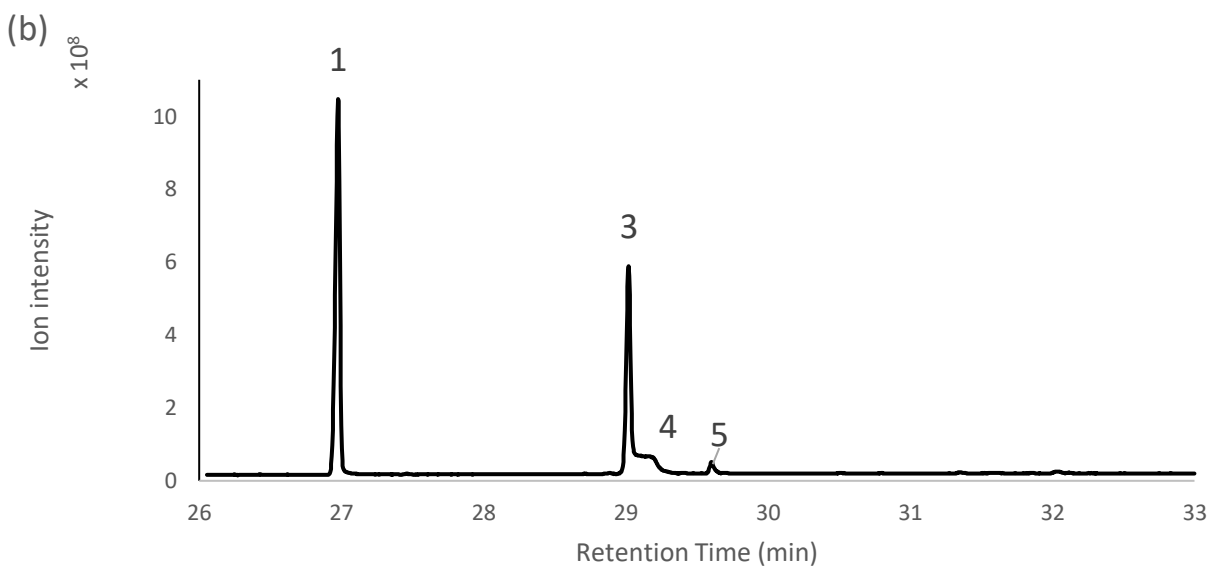
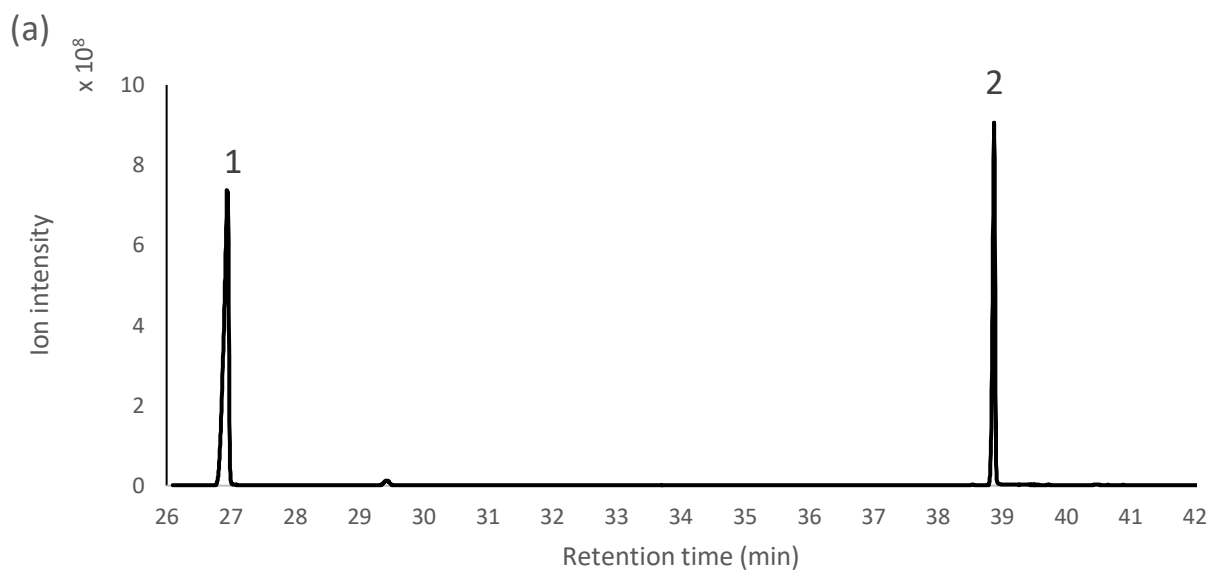


Fig. 3. 1 The total ion chromatograms from (a) polar fraction 1 and (b) polar fraction 2 of standards. Peaks are labelled as follows: 1) indicates internal standard (19:0); 2) indicate 9,10-epoxyoctadecanoate methyl ester; 3) indicates 13-HODE; 4) show an unidentified tail coeluted with peak 3 and 5) a peak identified as trans 13-HODE.

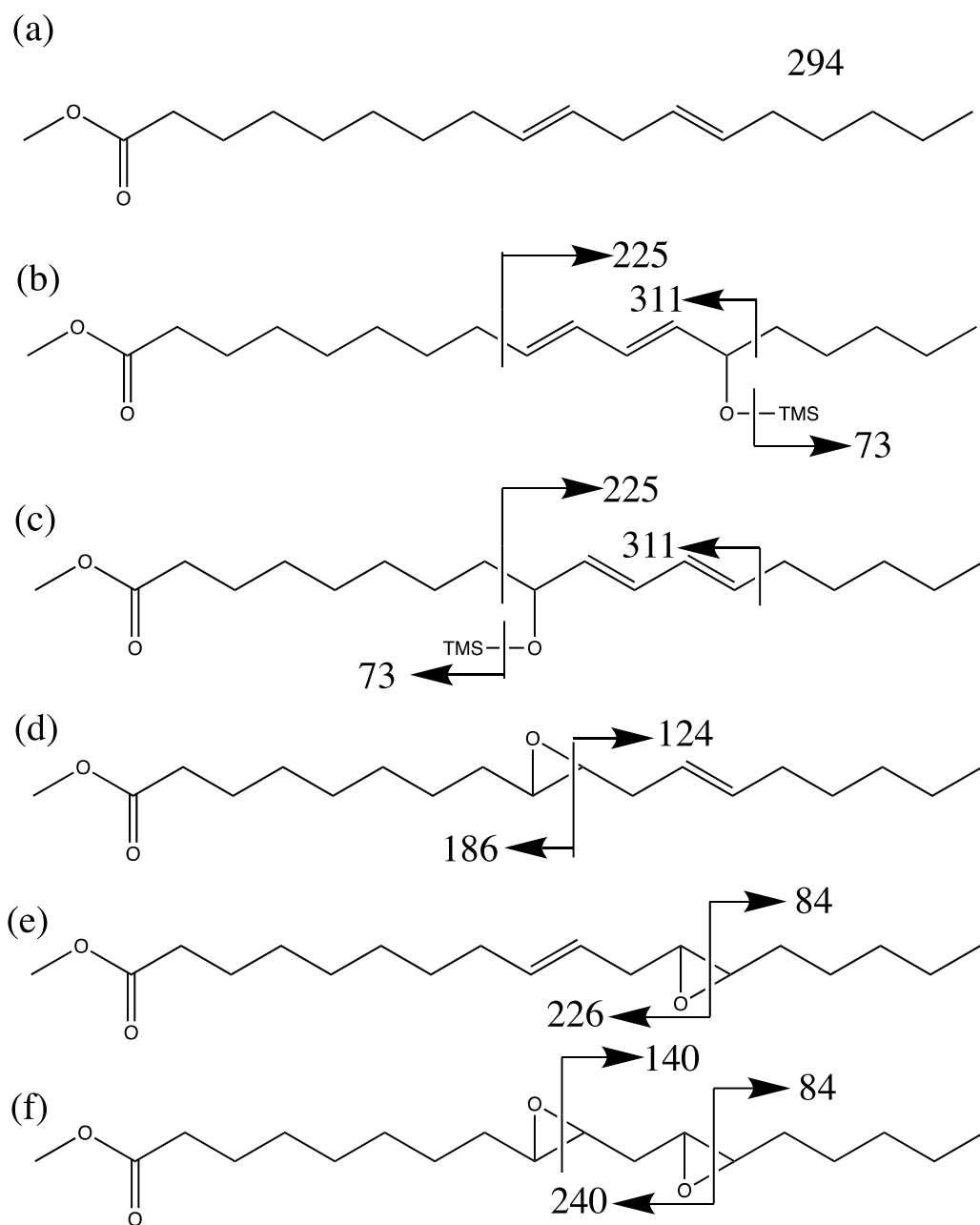


Fig. 3. 2 Electron ionization cleavage of (a) linoleic acid, (b) 13-HODE, (c) 9-HODE, (d) 9,10-epoxy-12-octadecenoic acid methyl ester, (e) 12,13-epoxy-9-octadecenoic acid methyl ester, and (f) 9,10-12,13-diepoxyoctadecenoic acid methyl ester. The structure of methyl nonadecanoic acid (internal standard) which has 312 m/z (molecular ion) as a characteristic peak is not presented.

3.1.2 Identification of Oxidation Products by GC-MS

GC-MS analysis showed several peaks in polar fraction 1, including the internal standard, epoxy-hydroxy FAME and an aldehyde. Polar fraction 2 chromatograms showed peaks representing internal standard, hydroxy FAME, epoxy-hydroxy FAME and an aldehyde (Fig. 3.3 and Table 2). Most of the linoleic acid methyl ester was eluted in the non-polar fraction, with only a very small portion present in polar fractions 1 and 2 which did not affect the identification and quantification of oxidation products. However, epoxy FAME were not detected in either polar fraction.

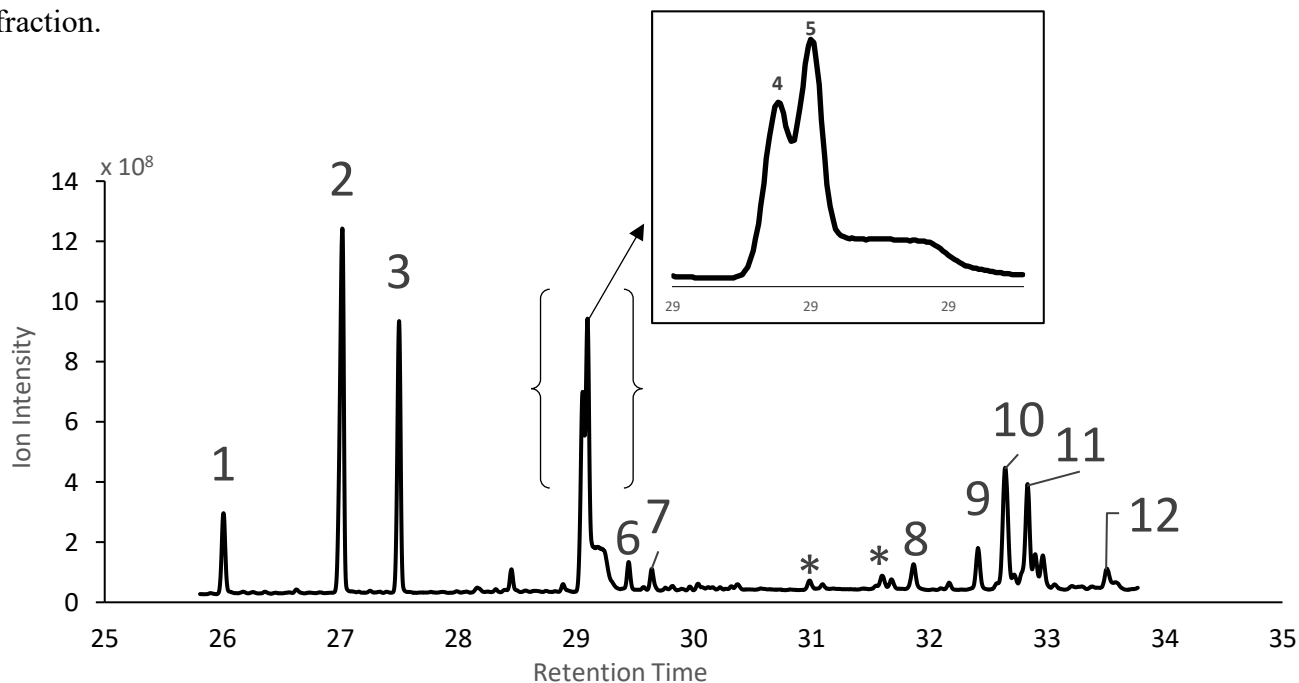


Fig. 3.3 GC-MS total ion chromatograms of aldehydes, hydroxy FAME TMS derivatives and hydroxy-epoxy FAME TMS derivatives in Polar Fraction 2 derived from trilinolein oxidized at 30 °C for 5 days, with peak identities listed in Table 2. * indicates unidentified TMS derivatives with 73 m/z ion mass in mass spectrum, suggesting that they were hydroxy compounds. The MS filament was on from 20 min to 53.8 min.

Internal standard and 13-HODE were identified by comparing the retention time and mass spectra of the standard mixture. The other compounds were identified using EI and PCI mass spectra since they were not available commercially. PCI-MS preserved the molecular ion of the compounds, yielding the molecular mass of each peak. By comparing the mass fragments in EI mass spectra to Fig. 1 and literature (Xia and Budge, 2017), the peaks were initially identified (Table 2). The aldehyde (peak 1) was identified as 9-oxo-nonanoic acid methyl ester by library match (NIST MS search 2.3) with over 95% probability (Fig. 3.4). The peaks labelled by * were small and could barely be detected in PCI mode. They were tentatively identified as monoacylglycerol with two TMS groups which the library indicated with over 90% probability.

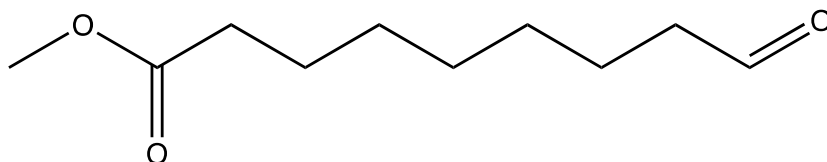


Fig. 3. 4 **Nonanoic acid, 9-oxo-, methyl ester**

Table 2 Identification of oxidation products in Polar Fraction 2 using spectra from both EI and CI modes, referring to the peaks labelled in Fig. 3.3

Peak No.	Compound	Molecular mass	Characteristic EI spectral ions m/z (Relative abundance%)
1	Nonanoic acid, 9-oxo-, methyl ester (Aldehyde)	186	74 (100), 87 (61), 83 (39)
2	Methyl nonadecanoic acid (internal standard)	312	74 (100), 87 (73), 312 (12)
3	Methyl linoleic acid	294	67 (100), 81 (96), 95 (72)
4,7 ^a	Methyl 13-hydroxyoctadeca-9,11-dienoate (13-HODE)	382	73 (100), 311 (30), 225 (20)
5,6 ^a	Methyl 9-hydroxyoctadeca-10,12-dienoate (9-HODE)	382	73 (100), 225 (47), 311 (14)
8,9,10,11,12 ^{ab}	Epoxy-hydroxy-FAME	398	73 (100), 129 (67), 285 (50), 199 (43)

^a Two peaks identified as the same compound were geometric isomers, showing identical mass spectrum but different retention times.

^b Five peaks labelled as 8,9,10,11,12 have identical mass spectra, suggesting that they were geometric isomers of the same compounds. The mass spectrum of peak 9 is shown in Fig. 6.

There was a flat tail on the 13-HODE peak (peak 3 in Fig. 3.1) and the major 9-HODE peak (peak 5 in Fig. 3.3) for both standards and samples. The mass spectra of the two tails in Fig. 1 and Fig. 3 were different (Fig. 3.5).

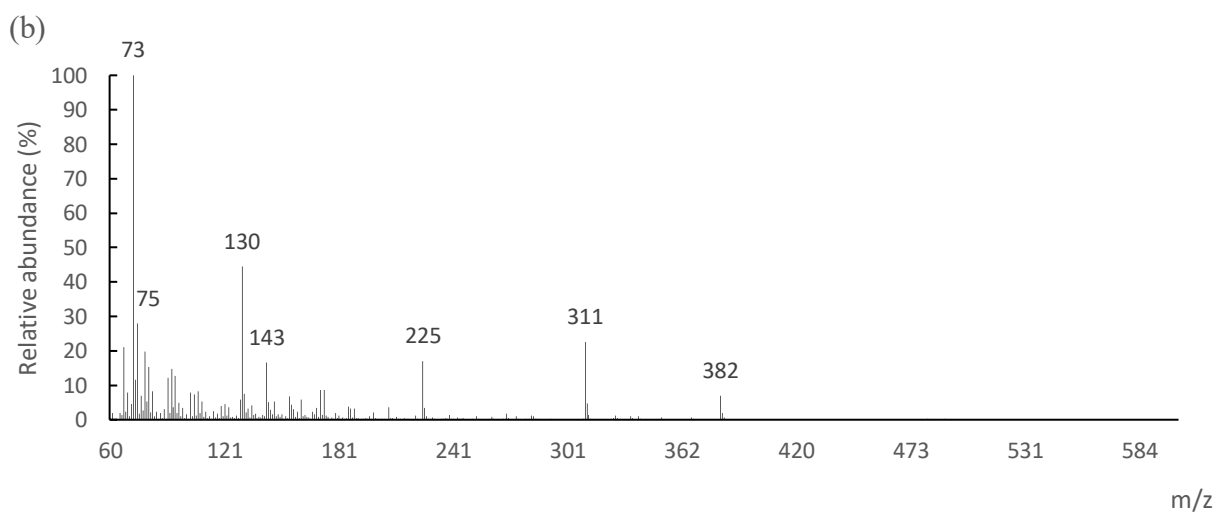
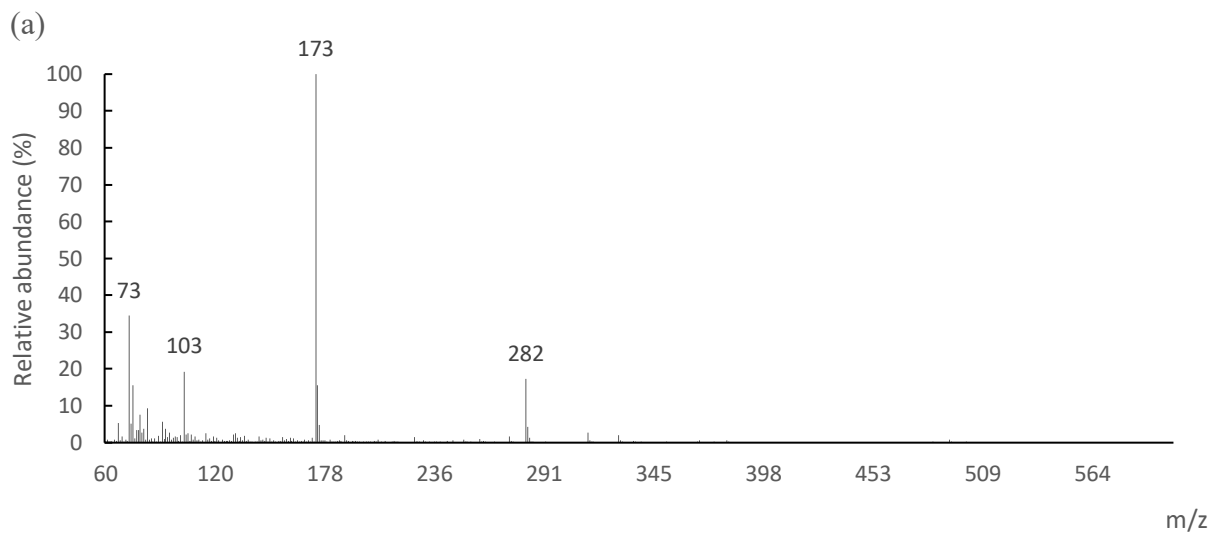


Fig. 3. 5^a EI mass spectrum of (a) tail of 13-HODE standard, (b) 13-HODE standard, (c) (d) tail of 9-HODE in sample and (e) 9-HODE in sample.

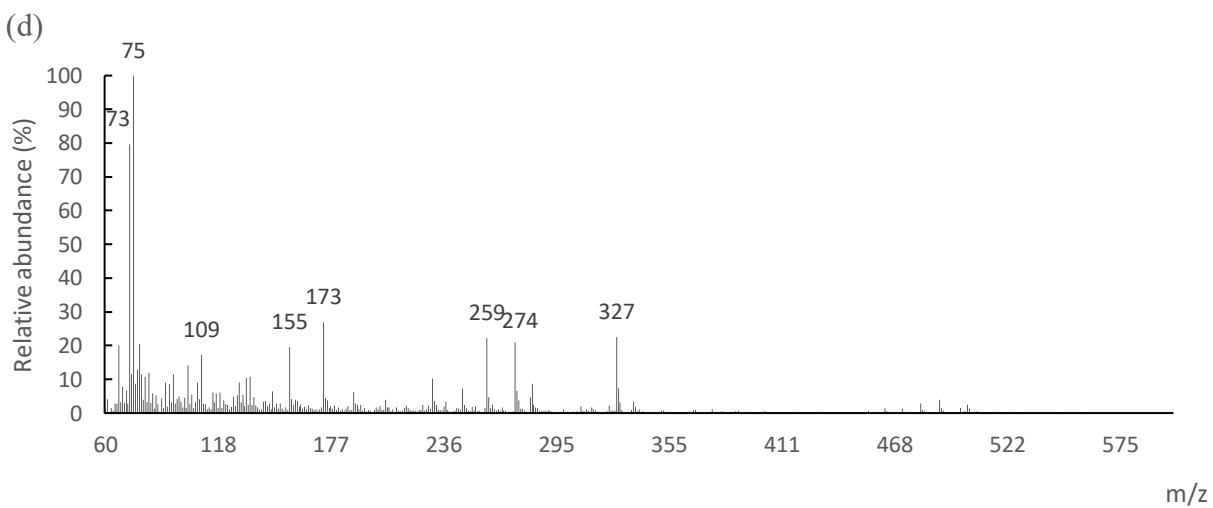
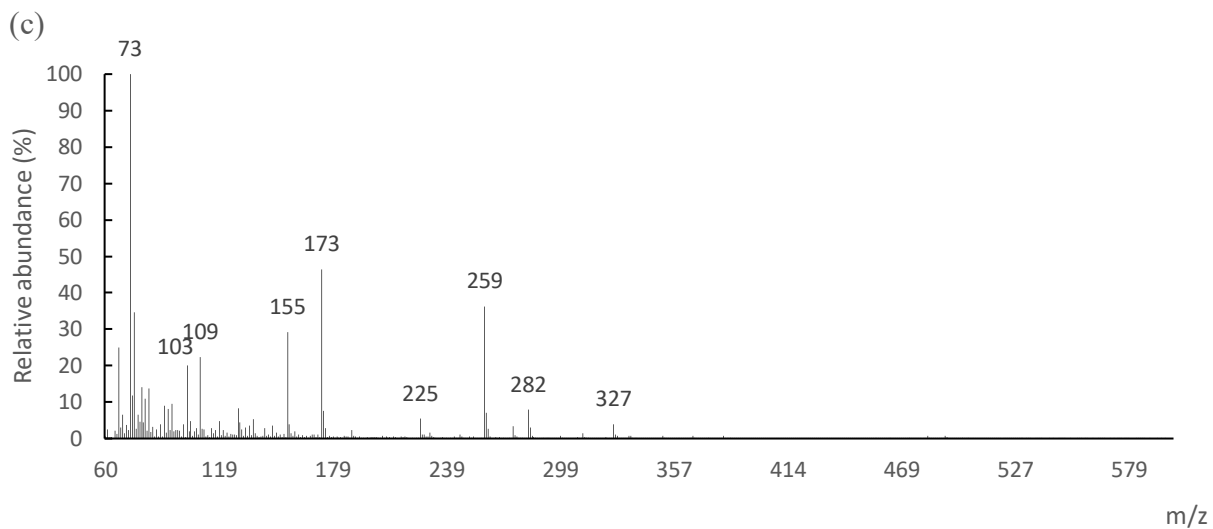


Fig. 3. 6^b EI mass spectrum of (a) tail of 13-HODE standard, (b) 13-HODE standard, (c) (d) tail of 9-HODE in sample and (e) 9-HODE in sample.

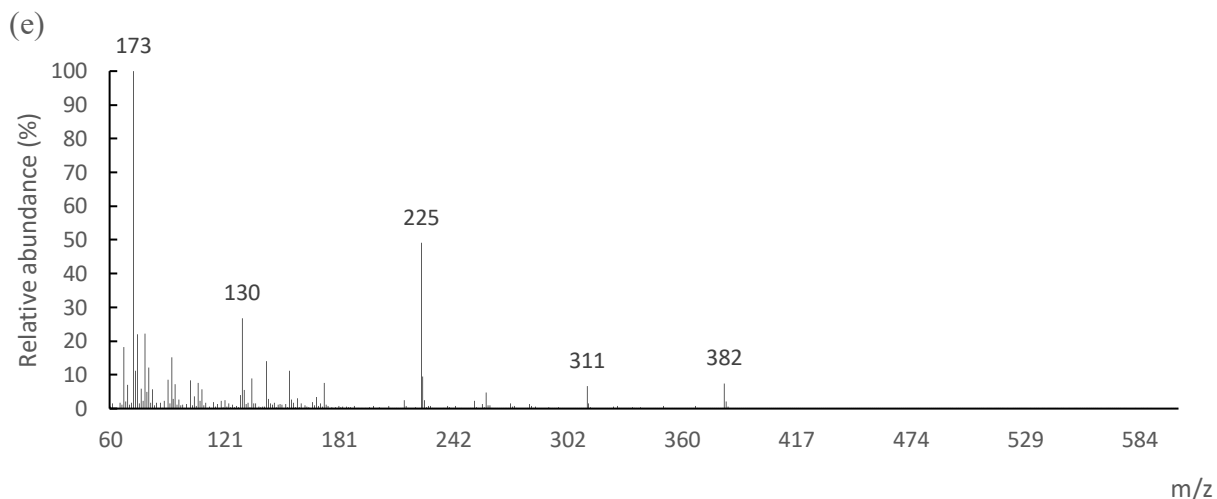


Fig. 3. 7^c EI mass spectrum of (a) tail of 13-HODE standard, (b) 13-HODE standard, (c) (d) tail of 9-HODE in sample and (e) 9-HODE in sample.

According to the EI spectra of the tails in chromatograms, several characteristic ions were apparent and included 155, 173, 225, 259, 282 and 327 m/z. PCI spectra of all tails in both standard and sample chromatograms indicated that they had the same molecular mass (382 m/z) as 13-HODE and 9-HODE. Thus, probable structures of radical ions produced during electronic ionization can be deduced (Fig. 3.6). The composition of the tails was believed to be a mixture of compounds whose structure consisted of single hydroxy functionalities bonded to different carbon atoms of an octadecadienoic acid methyl ester, including 14-hydroxy octadecadienoic acid methyl ester, 5-hydroxy octadecadienoic acid methyl ester and a geometric isomer of 9-HODE. There was likely to be decomposition and recombination of hydroxy functionalities and linoleic acid methyl ester during the oxidation of lipids which could lead to shifts in the position of the functionality. These tails were removed by peak optimization in the quantification procedure and are not included in concentrations of 13- and 9-HODE.

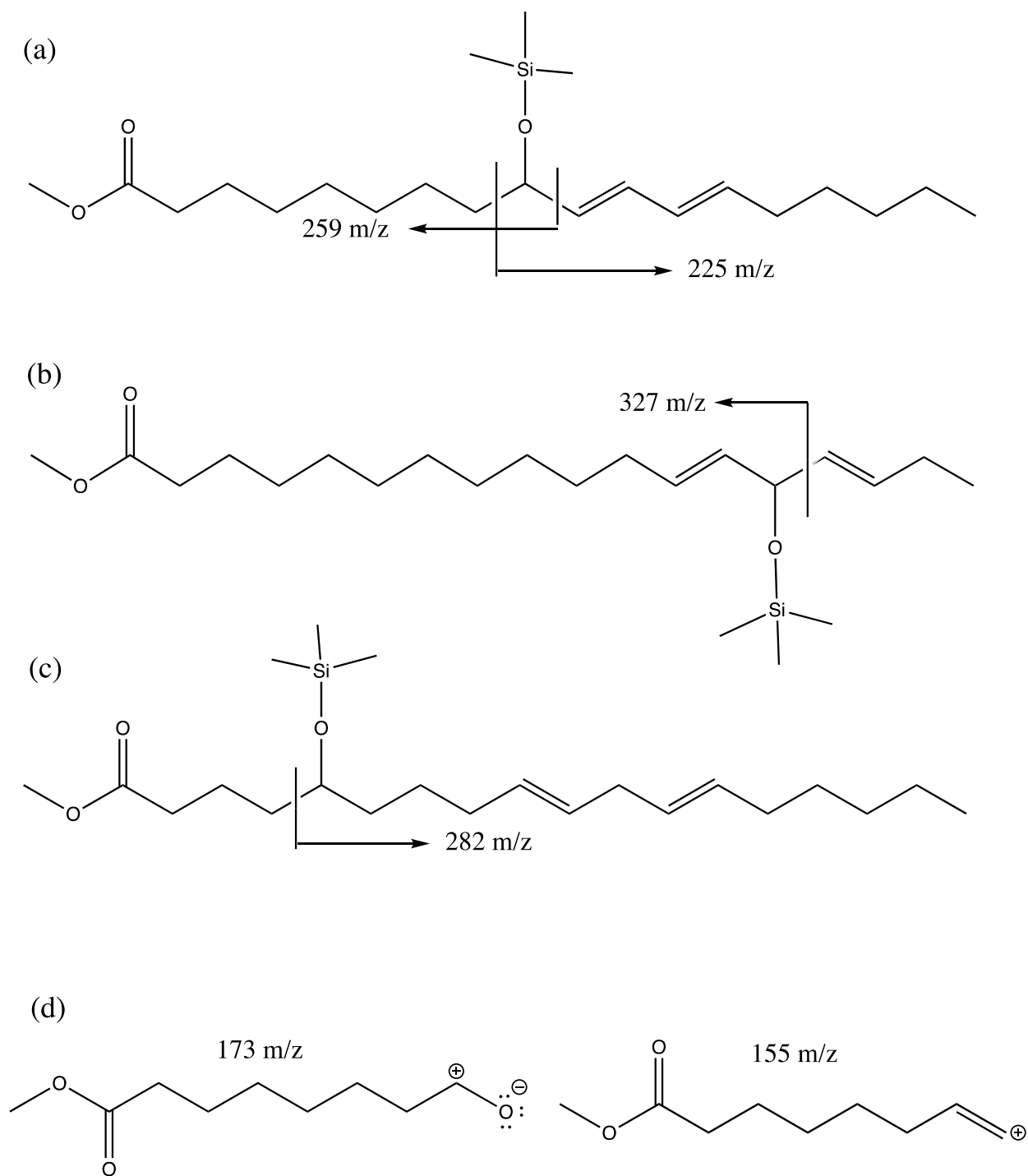


Fig. 3.8 Probable cleavage of (a) 9-HODE (b) 14-hydroxy octadecadienoic acid methyl ester, (c) 5-hydroxy octadecadienoic acid methyl ester and (d) two radicals with masses that match the ions peak in the spectra.

There were five peaks eluting from 32 min to 34 min (peaks 8,9,10,11,12 in Fig. 3.3) all of which had similar mass spectra (Fig. 3.7.). Their molecular masses were 398 m/z and they all had the same 199 m/z and 285 m/z mass peaks. This area of the chromatogram was highly consistent with the chromatogram Xia and Budge (2017) found. They suggested that they were epoxy-hydroxy-FAME. The two major structures are presented in Fig. 7. Since they co-eluted in the chromatograms, single ion chromatograms were plotted (Fig. 3.7) by monitoring m/z 199 and m/z 285 for methyl 13-OTMS-9,10-epoxyoctadec-11-enoate and methyl 11-OTMS-12,13-epoxyoctadec-9-enoate.

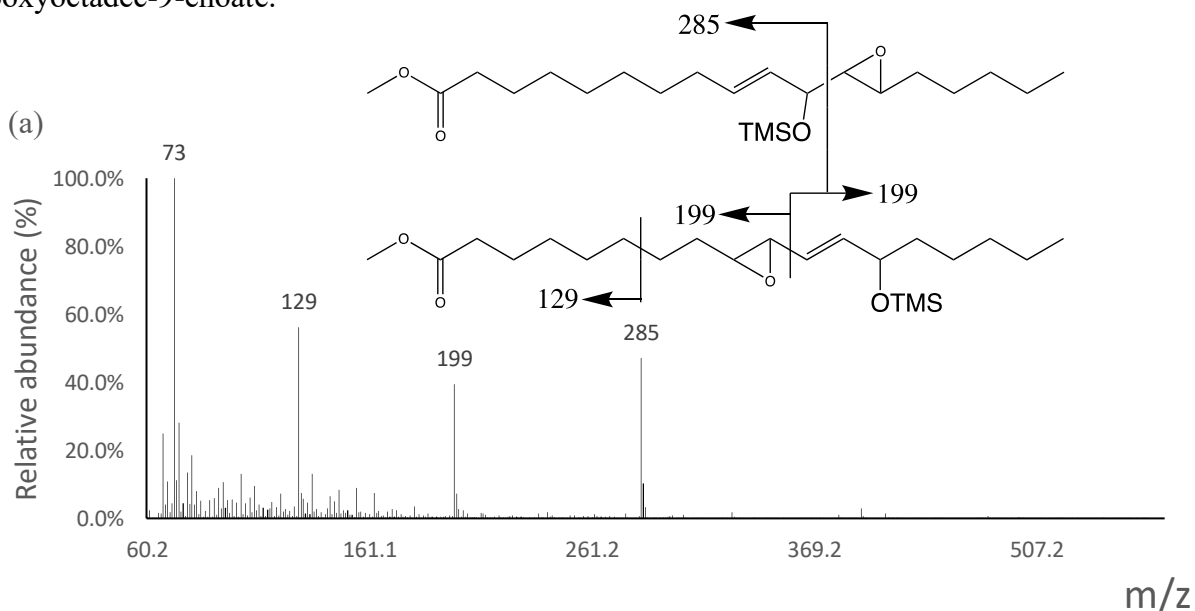


Fig. 3. 9^a Mass spectrum at EI mode (a) and PCI mode (b) of peak 9 in Fig. 1, suggesting that the compounds were co-eluting methyl 11-OTMS-9,10-epoxyoctadec-12-enoate and 11-OTMS-12,13-epoxyoctadec-9-enoate (both with molecular mass of 398). The m/z 285 ion arises from methyl 11-OTMS-12,13-epoxyoctadec-9-enoate and the 199 ion is derived from 11-OTMS-9,10-epoxyoctadec-12-enoate. Total ion chromatogram (c) and single ion chromatogram (d) of those compounds were also plotted.

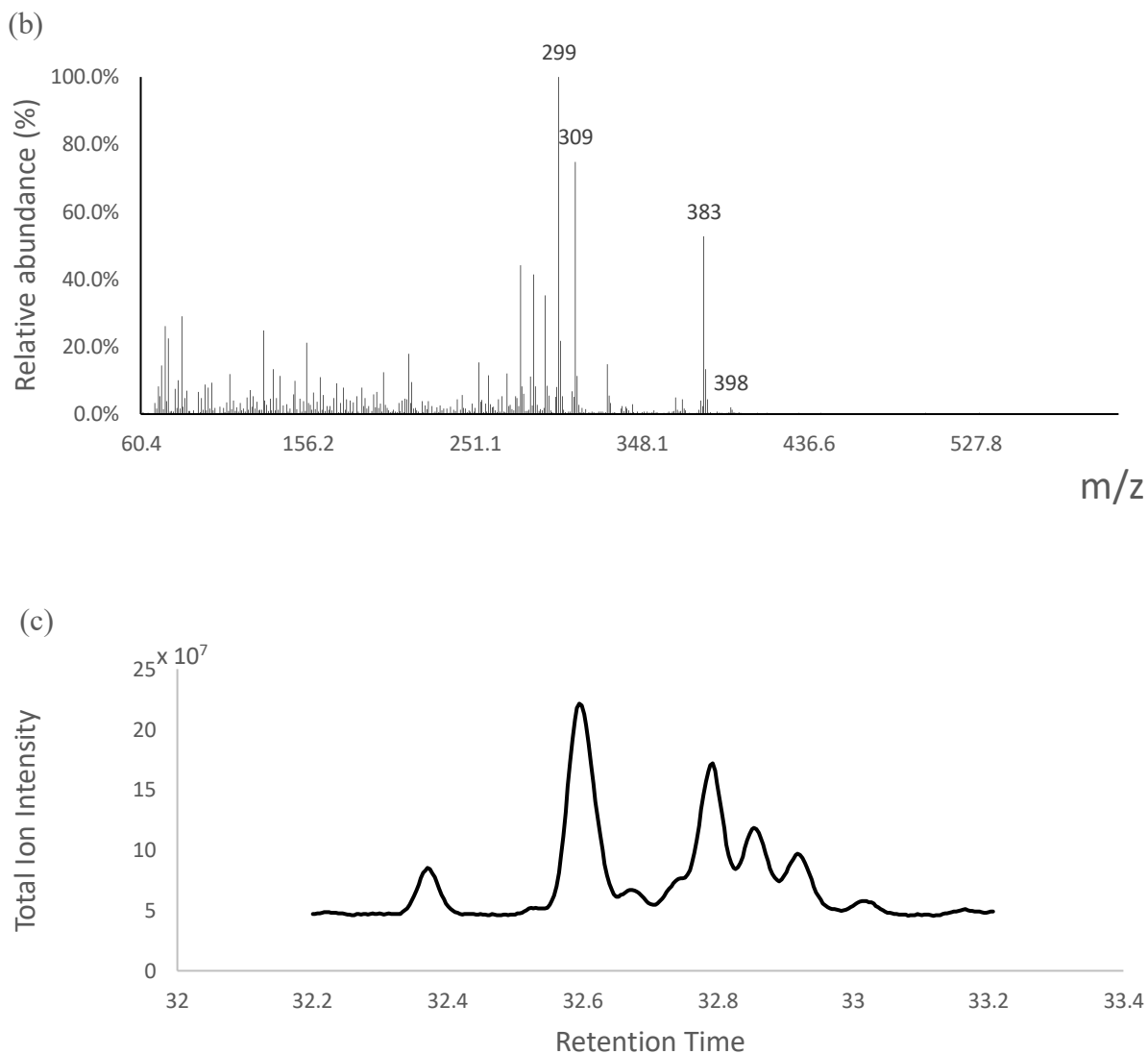


Fig. 3. 10^b Mass spectrum at EI mode (a) and PCI mode (b) of peak 9 in Fig. 1, suggesting that the compounds were co-eluting methyl 11-OTMS-9,10-epoxyoctadec-12-enoate and 11-OTMS-12,13-epoxyoctadec-9-enoate (both with molecular mass of 398). The m/z 285 ion arises from methyl 11-OTMS-12,13-epoxyoctadec-9-enoate and the 199 ion is derived from 11-OTMS-9,10-epoxyoctadec-12-enoate. Total ion chromatogram (c) and single ion chromatogram (d) of those compounds were also plotted.

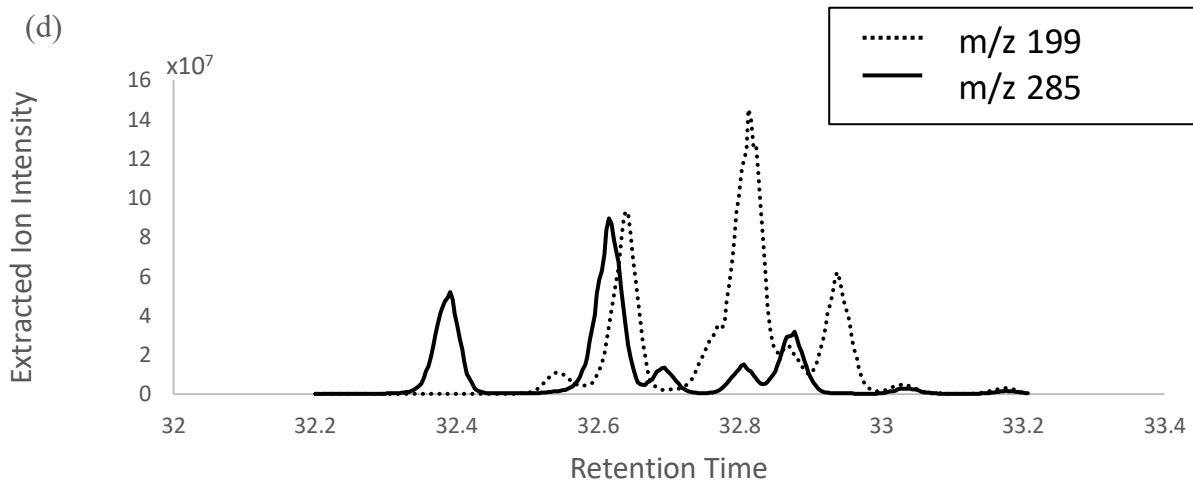


Fig. 3. 11^c Mass spectrum at EI mode (a) and PCI mode (b) of peak 9 in Fig. 1, suggesting that the compounds were co-eluting methyl 11-OTMS-9,10-epoxyoctadec-12-enoate and 11-OTMS-12,13-epoxyoctadec-9-enoate (both with molecular mass of 398). The m/z 285 ion arises from methyl 11-OTMS-12,13-epoxyoctadec-9-enoate and the 199 ion is derived from 11-OTMS-9,10-epoxyoctadec-12-enoate. Total ion chromatogram (c) and single ion chromatogram (d) of those compounds were also plotted.

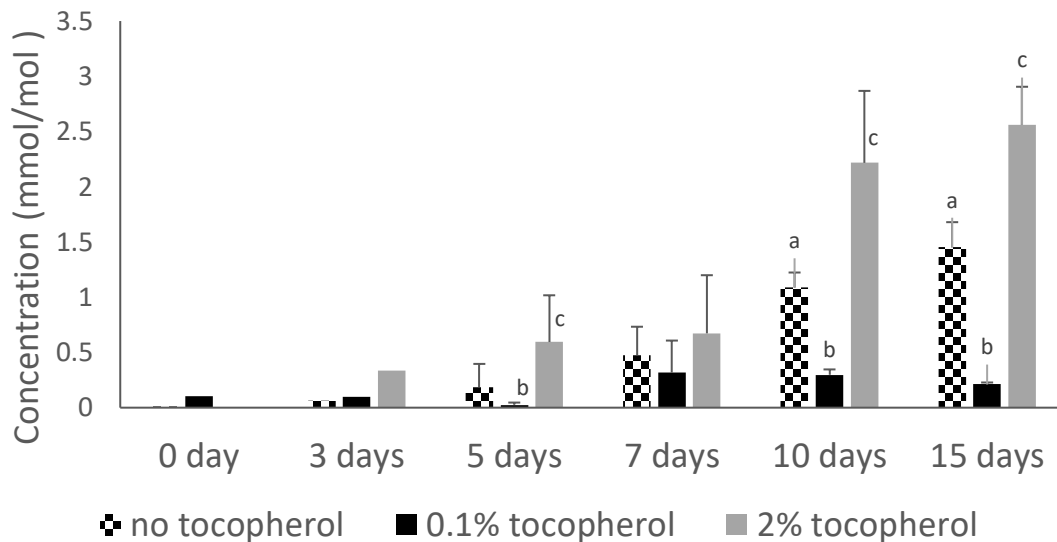
3.2 QUANTITATIVE ANALYSIS OF OXIDATION PRODUCTS IN OILS

Although epoxy FAME was not detected, 13-HODE, 9-HODE, aldehyde and epoxy-hydroxy FAME were quantified as oxidation products (mmol mol^{-1} Fig. 3.8). Since the tail consisted of positional isomers of 9-HODE, it was not included in the concentration of 9-HODE. However, the geometric isomers, *trans* 13-HODE and *trans* 9-HODE (peaks 6 and 7, respectively, in Fig. 3.3) were quantified as 13-HODE and 9-HODE. For all oxidation products, in comparison with the other groups, the concentration showed only minor fluctuations in samples treated with 0.1% tocopherol (Fig. 3.8) over the course of the oxidation period, which demonstrated that 0.1% tocopherol was an excellent antioxidant at that concentration. The concentrations of oxidation

products in samples without tocopherol and with 2% tocopherol showed an obvious increase in the 15-day experimental cycle (Fig. 3.8). For the 2% tocopherol treated group, the mean concentration of all oxidation products at a given time point tended to be higher than that of the control group, except for 9-HODE on day 15.

At the last two time points, there were significant differences (ANOVA; $p < 0.05$) among all groups for all compounds, except for 9-HODE on day 15 and epoxy-hydroxy FAME on day 10, for which there was no difference between the control and 2% tocopherol groups (Fig. 3.8). In the first half of the experimental cycle, there was insufficient statistical evidence to demonstrate real differences between the three groups for all compounds.

(a) 13-HODE



(b) 9-HODE

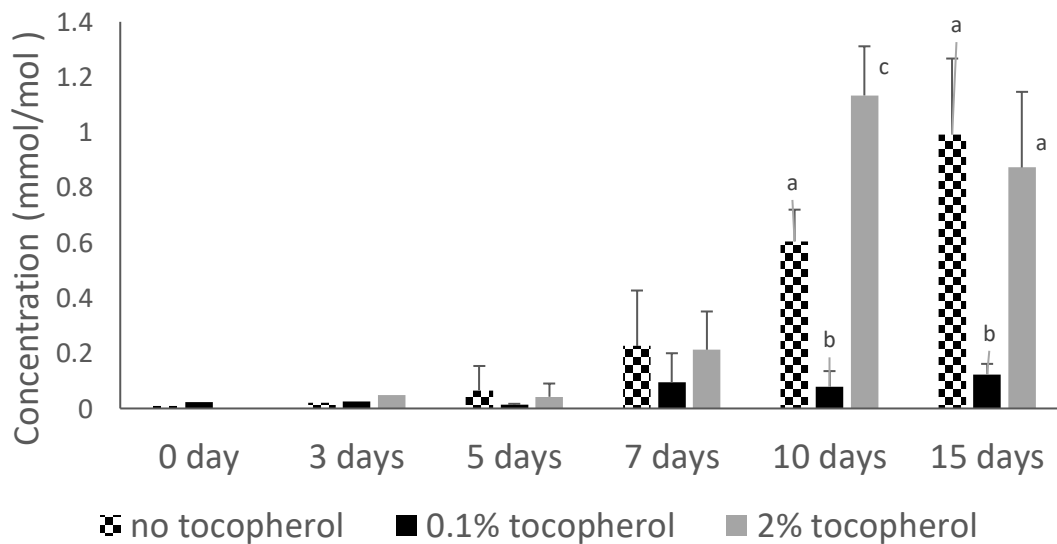
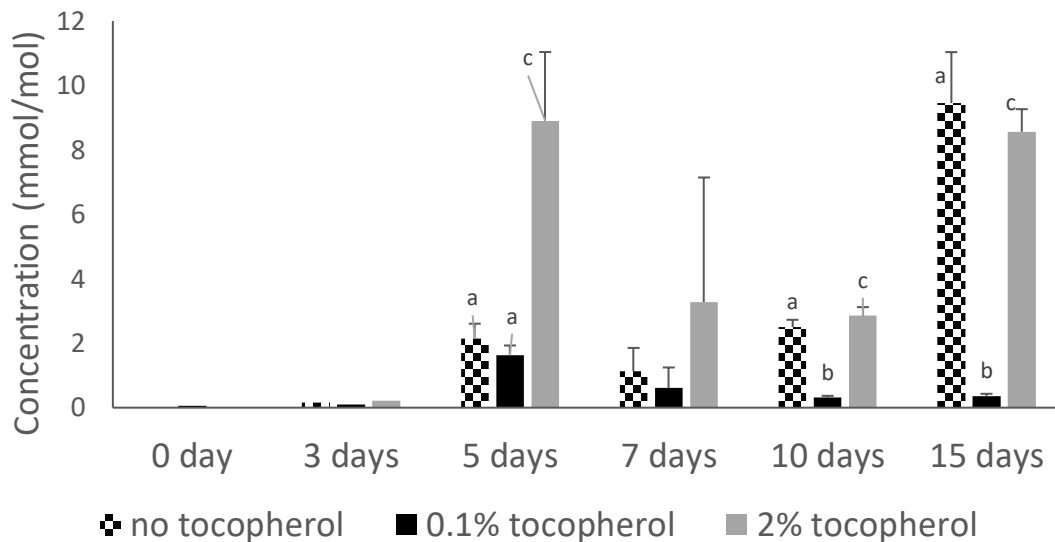


Fig. 3. 12^a Mean concentrations and standard deviations of (a) 13-HODE, (b) 9-HODE, (c) aldehyde and (d) epoxy-hydroxy-FAME in oxidized linoleic acid methyl ester at different time points quantified by GC-FID. At each sampling time, different letters indicate significantly different concentrations (ANOVA; n=3; p < 0.05).

(c) Aldehyde



(d) Epoxy-hydroxy FAME

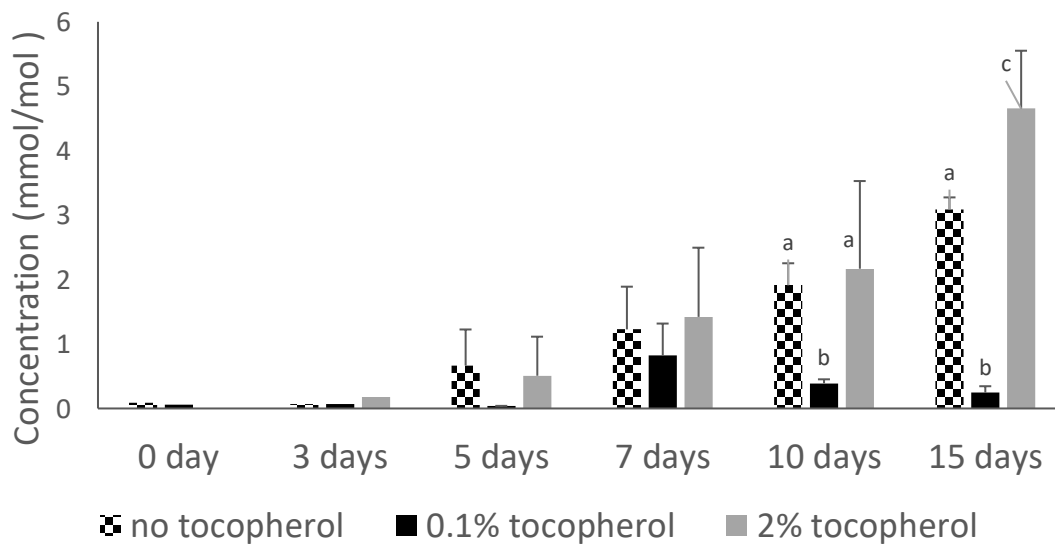


Fig. 3. 13^b Mean concentrations and standard deviations of (a) 13-HODE, (b) 9-HODE, (c) aldehyde and (d) epoxy-hydroxy-FAME in oxidized linoleic acid methyl ester at different time points quantified by GC-FID. At each sampling time, different letters indicate significantly different concentrations (ANOVA; n=3; p < 0.05).

3.3 MODELING OF OXIDATION RATE

Samples treated with 2% tocopherol consistently had similar slopes and therefore similar oxidation rates as the control group without tocopherol (Table 3); the 0.1% tocopherol group always had more gradual slopes indicating the best antioxidant capacity (Fig. 3.9). Because the regression line for the 2% tocopherol group for all oxidation products, except the epoxy-hydroxy FAME, had a greater intercept and shallower slope, given sufficient oxidation time, it would intersect the regression of the control group. Thus, the prooxidant capacity of α -tocopherol, relative to the control, seems to be reduced as the concentration of oxidation products or duration of oxidation increases. However, two-sample t-tests only indicated significant differences in oxidation rates between the control group and 0.1% tocopherol group for 9-HODE and aldehydes. The high standard deviation on the individual time points and the large range of confidence intervals undoubtedly influenced the results of statistical analysis, despite what appears to be obvious difference.

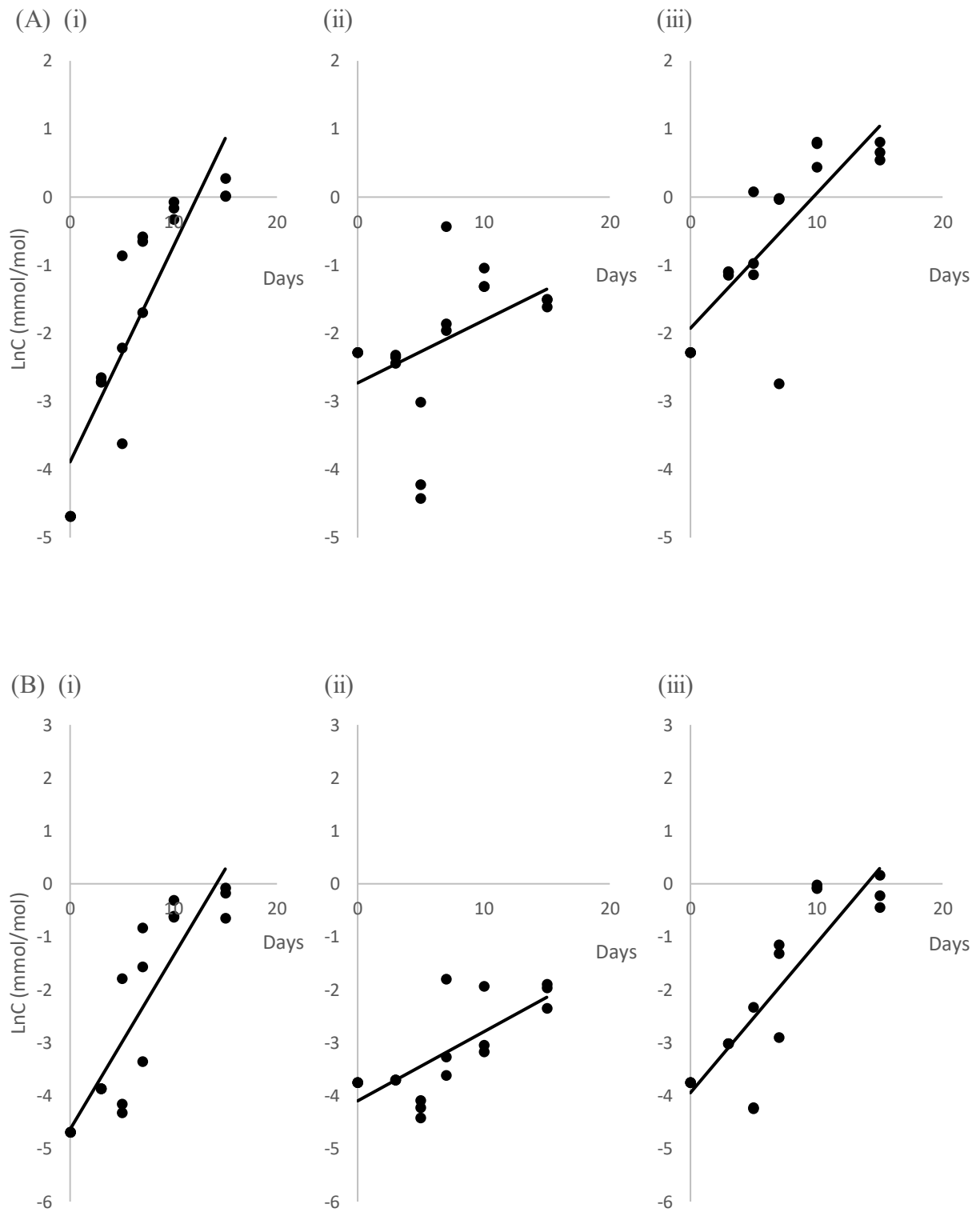


Fig. 3. 14^a Oxidation rate model of 13-HODE and 9-HODE

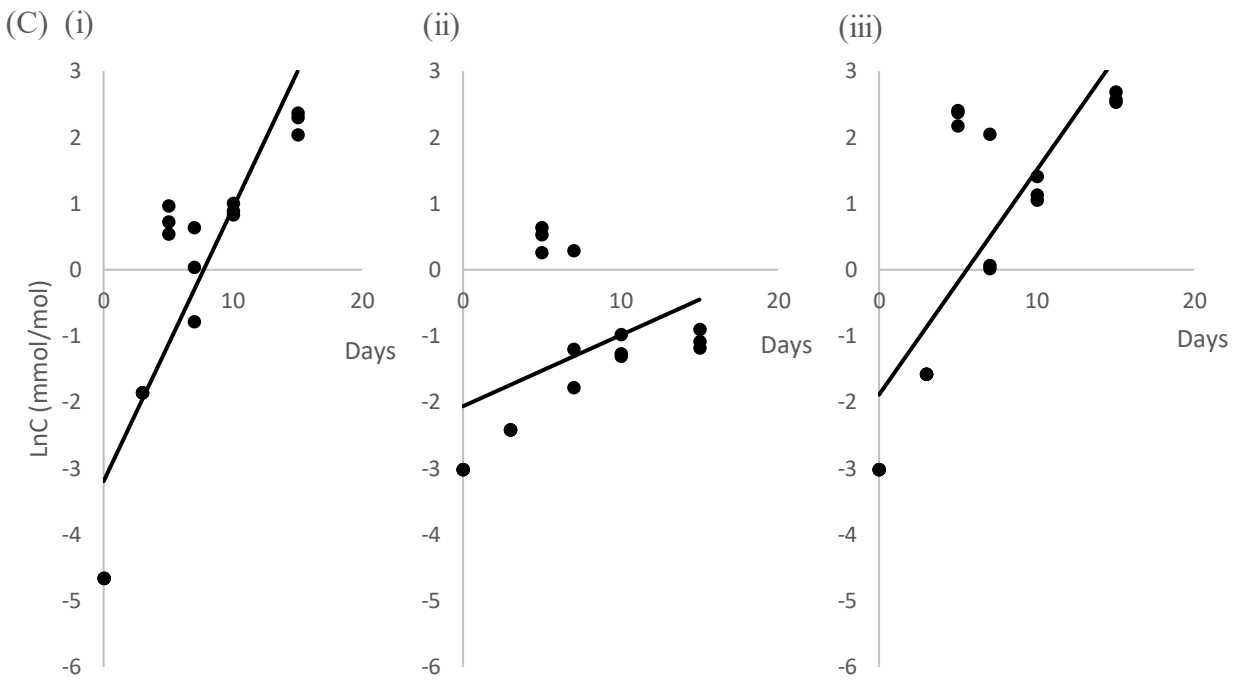


Fig. 3.15^b Oxidation rate model of Aldehyde

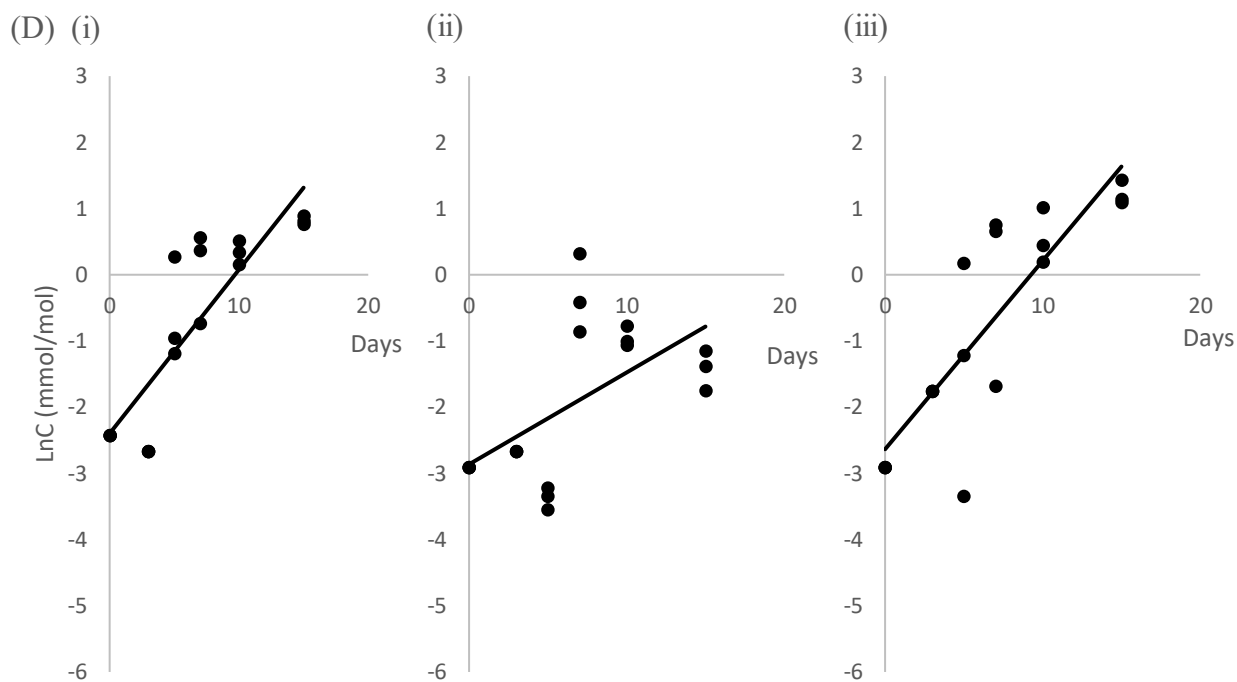


Fig. 3.16^c Trendline fitted by natural logarithm of the initial concentration of (A) 13-HODE, (B) 9-HODE, (C) aldehydes and (D) epoxy-hydro-FAME in linoleic acid methyl ester during 15-day experimental cycle. Data are fitted with Equation 2.2 and corresponding parameters are found in Table 3. The samples treated with no tocopherol, 0.1% tocopherol and 2% tocopherol were labelled as (i), (ii) and (iii) respectively. The dotted lines show the confidence intervals of their oxidation rates (k in equation 2.1).

Table 3 Estimates of oxidation rates (k) and their confidence interval of groups treated with tocopherol at different concentrations derived from the exponential model fit to the data obtained. For an oxidation product, mean values with different superscripts are significantly different (pooled variance t-test; p<0.05).

Oxidation Products	Group	k (days ⁻¹)
13-HODE	no tocopherol	0.32±0.08 ^a
	0.1% tocopherol	0.09±0.09 ^b
	2 % tocopherol	0.20±0.08 ^b
9-HODE	no tocopherol	0.33±0.09 ^a
	0.1% tocopherol	0.13±0.06 ^b
	2 % tocopherol	0.28±0.09 ^a
Aldehydes	no tocopherol	0.41±0.12 ^a
	0.1% tocopherol	0.11±0.12 ^b
	2 % tocopherol	0.34±0.14 ^a
Epoxy-Hydro-FAME	no tocopherol	0.25±0.08
	0.1% tocopherol	0.14±0.10 ^a
	2 % tocopherol	0.28±0.09 ^b

CHAPTER 4 DISCUSSION

4.1. IDENTIFICATION OF OXIDATION PRODUCTS

Trilinolein was adopted as the substrate in this research so that the pathways of formation of all the oxidation products could be deduced, since they are all derived from the same initial reactant. The oxidation of this pure triacylglycerol led to the formation of four major oxidation products that were subsequently characterized using the optimized SPE procedure established by Xia and Budge (2017) for the separation of hydroxy and epoxy FAME in oxidized vegetable oils. Under Xia and Budge (2017)'s experimental parameters, all the peaks in the chromatograms were identified successfully. In agreement with previous literature (Xia and Budge, 2017; Martin-Rubio et al., 2018; Marmesat et al., 2008), in the current study, hydroxy FAME, epoxy-hydroxy FAME and aldehydes were identified as oxidation products. Although reported in other work, epoxy FAME and intact keto FAME were not formed here which was likely the result of different reactants, shorter oxidation times, lower temperatures of thermo-oxidation parameters and the influence of α -tocopherol. Other studies which have reported their appearance used vegetable oils as samples with more than 70 °C and 20 days as thermal oxidation parameters (Martin-Rubio, 2018); further, tocopherols were not added to the samples (Marmesat et al., 2008; Xia and Budge, 2018; Grüneis et al., 2019). The reactant is probably most important, with epoxy FAME and keto FAME more likely to form from monounsaturated lipid instead of linolein. There is a great possibility that polyunsaturated lipids would form epoxy-hydroxy FAME directly during oxidation, skipping the step producing epoxy FAME. The possible pathways of oxidation product production will be discussed below.

For hydroxy lipids, 13-HODE, 9-HODE and their geometric isomers were identified following the mass spectrum as Xia and Budge (2018) showed. However, in oxidized trilinolein, we detected several HODEs with different structures but the same molecular mass (382 m/z) which were not mentioned in previous literature. Their mass spectra indicated that the hydroxy functionalities were likely to be bonded to the 5th and 14th carbon atoms in the chain. Specific pathways for the formation of these two HODEs have not been described but since they were also identified in the commercial 13-HODE standard, they were very likely produced from 13-HODE and 9-HODE instead of direct oxidation of linoleic acid. Hypothetically, during the lipid oxidation period, hydroxy octadecadienoate methyl ester could undergo decomposition and recombination which could change the position of the hydroxy group. Although oxidation products with two structures were identified, they remained unresolved as a shoulder in the chromatograms. Thus, 14-HODE and 5-HODE might not be the only HODEs present in the standard and samples. Separation and identification of all the structures in that shoulder is necessary to postulate logical pathways of their production.

To attempt that separation and eventual identification of all the HODEs, a DB-23 column was installed on the GC since Xia and Budge (2017) found it a useful phase for separation of hydroxy FAME. Unfortunately, separation was not improved relative to the RTX-2330, with the tails continuing to co-elute with the 9-HODE peak. Another phase, a longer column or a new optimized temperature program/flow rate might improve the separation and should be pursued in future work.

Epoxy-hydroxy FAME were common secondary oxidation products. Methyl 13-OTMS-9,10-epoxyoctadec-11-enoate and methyl 11-OTMS-12,13-epoxyoctadec-9-enoate were also

identified by Xia and Budge (2018) in oxidized vegetable oils whose major fatty acid was 18:2n-6. However, 18:1n-9 and 18:3n-3 were also present at 59.76% and 9.35% (w/w total FAME), respectively, in canola oil. Thus, to gain a better understanding of the pathways leading to formation of epoxy-hydroxy FAME, use of a single substrate was necessary. Two pathways describing formation of epoxy-hydroxy FAME produced have been published. Hamberg and Gotthammar (1973) believed epoxy-hydroxy FAME were created by the cleavage and recombination of hydroperoxides while Xia and Budge (2017), suggested that it was produced from epoxy FAME (Fig. 4.1). Although Either pathways could explain the transformation from 18:2n-6 to epoxy-hydroxy fatty acids, the hydroxy functional group was considered generating first due to the fact that there was no epoxide identified in chromatograms. The pathway provided by Raghavamenon et al. (2009) (Fig. 4.2) is the closest one to the results in this study.

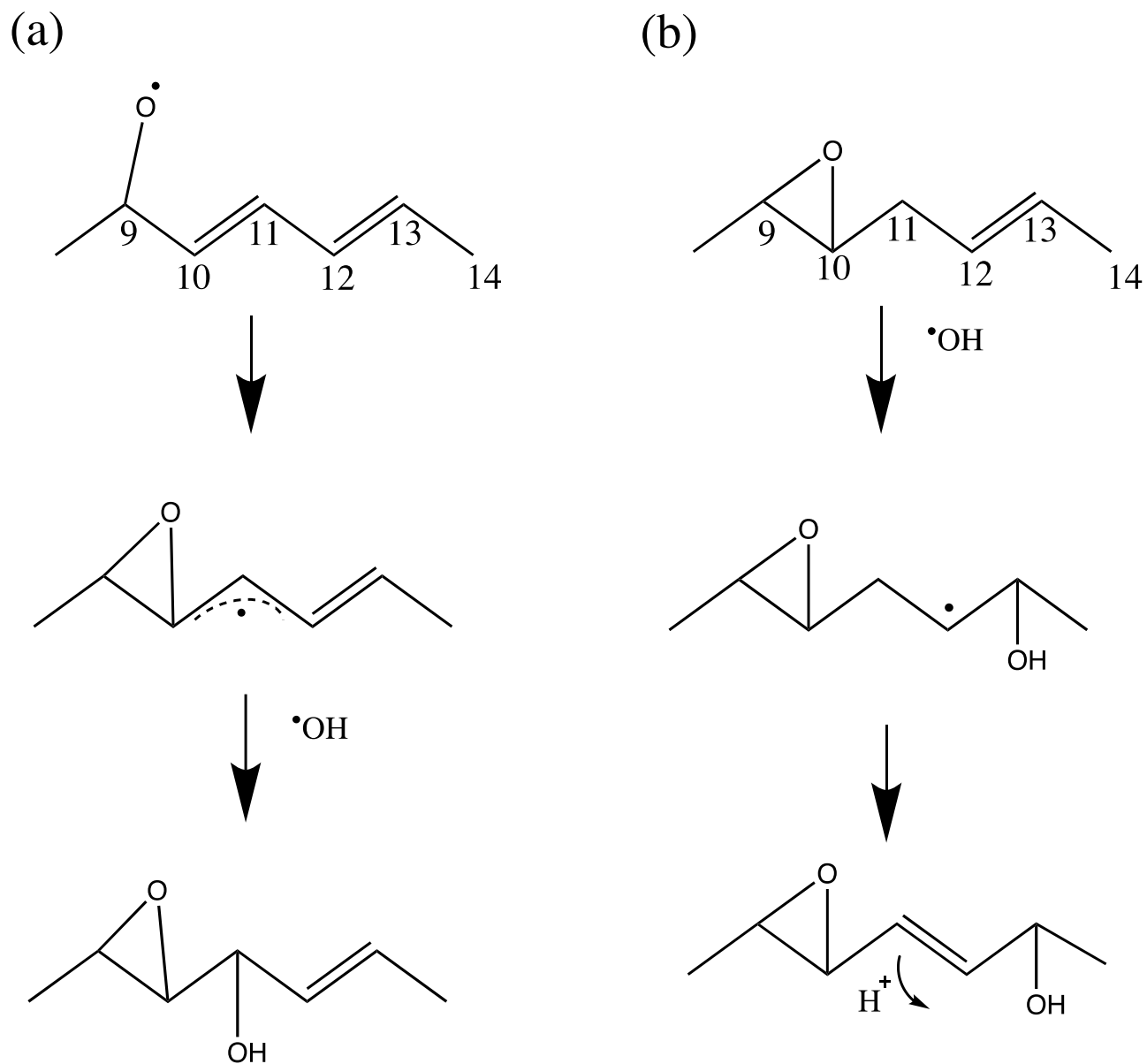


Fig. 4.1 Two probable pathways can produce epoxy-hydroxy FAME from (a) hydroperoxides and (b) epoxides during oxidation.

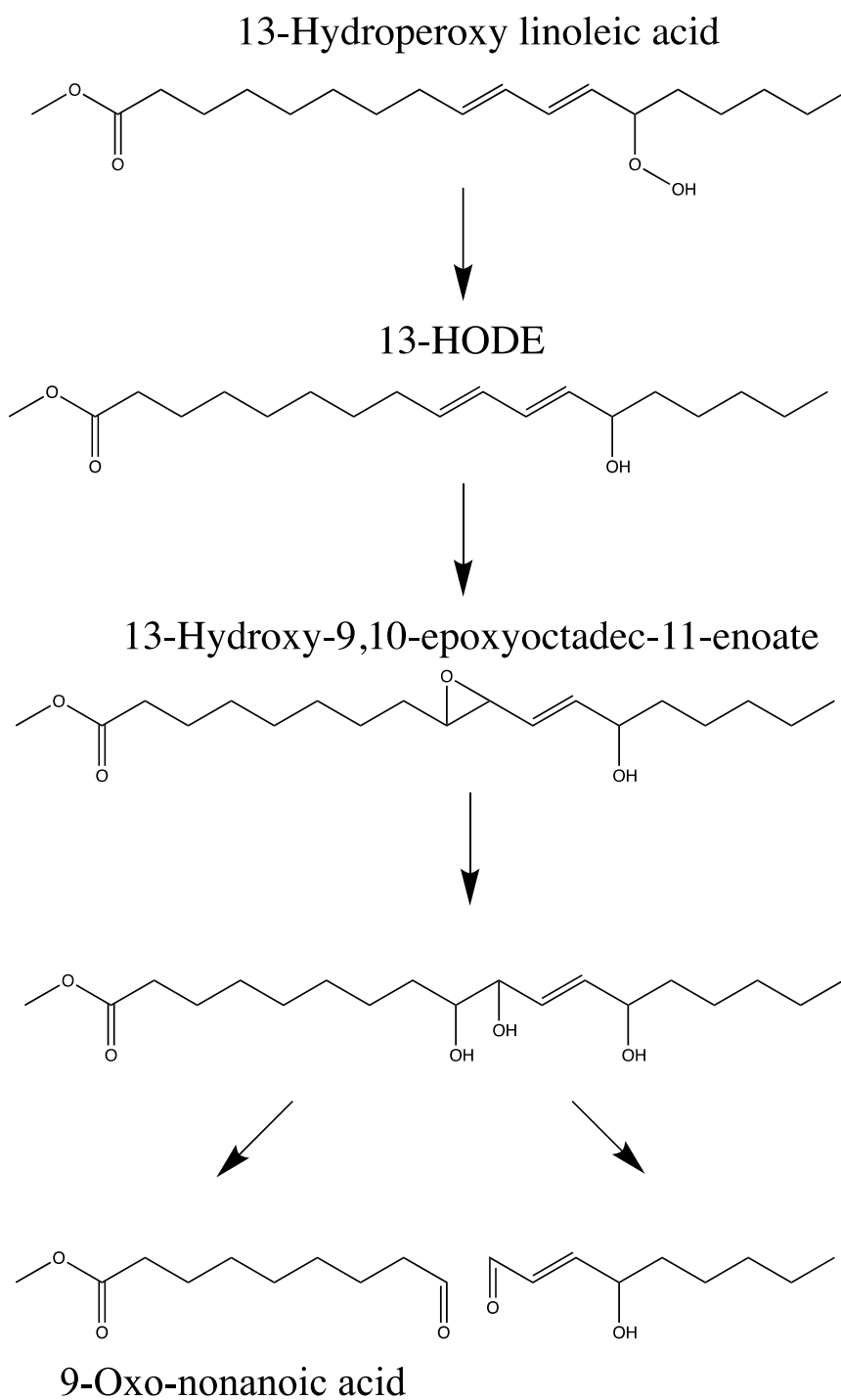


Fig. 4.2 Hydroperoxides decompose following a mechanism that proceeds through hydroxy-epoxy structures to end with the formation of aldehydes (Raghavamenon et al., 2009).

The aldehyde in the sample was identified by library spectra matching as 9-oxo-nonanoic acid methyl ester. Like the epoxy-hydroxy FAME, Gardner et al. (1974) suggested that it too was produced through hydroperoxide decomposition (H.W. Gardner et al. 1974) (Fig. 4.3). Research that followed considered a pathway in which aldehydes were produced by the breakdown of epoxy-hydroxy FAME (Fruebis et al., 1992) (Fig. 4.2). Aldehydes are highly volatile compounds, with most likely lost during the thermo-oxidation procedure in open vials; an aldehyde produced by cleavage at the 'b' position in Fig. 4.3, creating structure (b), would be unlikely to be identified for that reason. However, cleavage at the 'a' position would generate an oxo-methyl ester similar to structure (a); since this aldehyde was originally bonded to the glycerol backbone, its volatility would be reduced. That explains why we did not detect structure (b) and confirms the reliability of quantifying structure (a) as an oxidation product.

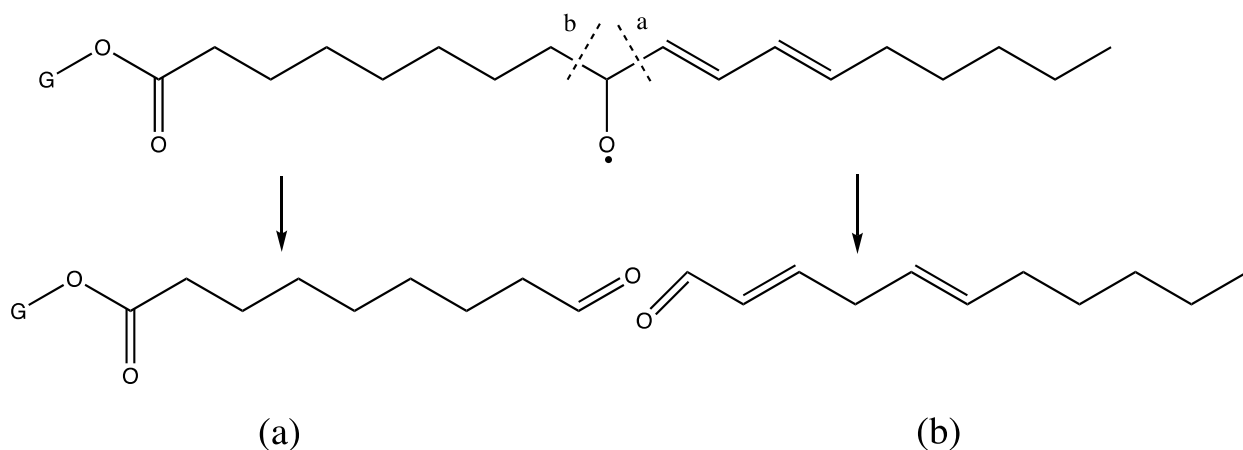


Fig. 4.3 Two products are derived from the decomposition of a peroxide radical. G indicates diacylglycerol backbone.

4.2. QUANTIFICATION OF OXIDATION PRODUCTS

In the chromatogram of the 13-HODE standard, the appearance of tail 4 and unexpected peak 5 (Fig. 3.1) suggested that during long-term storage, a small portion of 13-HODE was degraded. Thus, the true amount of 13-HODE in the calibration curves is actually less than thought, leaving the regression with an erroneously steep slope and generating concentrations for 13-HODE that would be overestimates. Also, during integration of the chromatograms, all the peak areas were auto-optimized by the software, which excluded the shoulder of 9-HODE in quantification. According to the EI mass spectra of the shoulder, some small portion of it consisted of a 9-HODE geometric isomer. Therefore, similar to the results for 13-HODE, the concentration of 9-HODE was likely to be lower than true. However, the calibration curves incorporating the small errors were applied to all the data in this study so that all samples were affected in the same fashion, allowing them to be compared.

The variation in replicate data for all oxidation products was large. This is a direct result of the experimental design. In order to maintain independent samples, each replicate was oxidized in an individual vial so that each vial experienced slightly different oxidation conditions, contributing to the variation observed here. A different design where samples are withdrawn from the same container would eliminate this problem; however, while common, that design suffers from pseudo-replication and underestimates the true variation in oxidation. The sample preparation prior to GCMS analysis also involved multiple steps and likely contributed to the variation within replicates. The large variation affected the analysis, leading to few statistical differences in the data between groups treated by 0.1% and 2% tocopherol, although there was an obvious trend in

Fig. 3.8 and Fig. 3.9. Therefore, to deal with this variation, more samples and replicates are needed. Based on the original experimental design, adding another 3 replicates from one container would likely be an effective solution in future work. In other words, the new replicates and the original replicates would be analyzed simultaneously, with the combined results having lower variation. Although statistical differences would still be difficult to detect due to pseudo-replication, the difference and relative trends among each group and oxidation products would be more obvious; further, such pseudo-replication would not influence the results of the pathways' analysis.

The chemical reaction rate was evaluated by converting the exponential curve into a linear regression curve to allow for a better comparison of the oxidation rates. In this way, the rates of reaction were assumed to be constant during the whole oxidation process. However, the real oxidation process was complex and the oxidation rates were likely to be continuously changing. The data points drawn by natural logarithm of concentration and time (Fig. 3.9) clearly were not fitted well to the linear model. There are several possible explanations for the inconsistent oxidation rates: 1) the consumption of antioxidants (tocopherols) was likely to change the oxidation rate; 2) the formation and decomposition of four major oxidation products proceeded simultaneously; and 3) the concentration of lipid reactant was reduced during the oxidation process. Thus, other models, such as a cubic regression might be more appropriate as an oxidation rate model. In a cubic model, although oxidation rates could be compared between groups at each time point, they are still speculations because of the simultaneous formation and decomposition of oxidation products. For simplicity, a logarithm model, based on first order kinetics, was therefore adopted in this research. In other words, the oxidation rates reported here represent a speculation for comparison rather than accurate oxidation rates.

4.3 THE INFLUENCE OF ALPHA-TOCOPHEROL ON OXIDATION PATHWAYS

4.3.1 The Antioxidant and Prooxidant Capacity of α -Tocopherol

Oxidation products in 0.1% tocopherol-spiked oil were always at lowest concentration and reaction rate compared to the other two groups during the whole experimental cycle (Fig. 3.8 and Fig. 3.9), which provided statistical evidence for the excellent antioxidant capacity of 0.1% α -tocopherol. A mechanism for the antioxidant activity of phenolic compounds was suggested in great detail by Frankel (2005) and that of tocopherol is similar; it functions by donating hydrogen atoms and producing stable radicals, which would be delocalized instead contributing to chain propagation. Hence, the tocopherol would interfere with the formation of hydroperoxides, the primary oxidation products.

When plotted as regressions, it becomes clear that there is a trend for concentrations of 13-HODE, 9-HODE and aldehydes in the 2% tocopherol-spiked oil to start at higher concentrations but increase at a lower rate than the control oil, so that at some point in the future, the concentrations of 13-HODE, 9-HODE and aldehydes in the control oil would exceed those of the 2% tocopherol-spiked oil. In other words, oxidation products in the 2% tocopherol group formed earlier than in the control group, which demonstrated tocopherol's prooxidant capacity, as other studies have noted (Kulås et al., 2002; Romero et al., 2004; Martin-Rubio et al., 2018). Although Frankel (2005) did not provide a description of the prooxidant mechanism specifically for α -tocopherol, he suggested that there was prooxidant activity for all phenolic antioxidants and offered a general mechanism that can be applied to tocopherol. Normally, after initiation, autoxidation produces radicals and they react preferentially with α -tocopherol to produce stable structures. At high concentrations, tocopherol would be oxidized first, producing tocopherol

radicals that have a tendency to act as chain-carriers by propagating new radicals, and thereby become prooxidants (Fig. 4.4). With the increase in tocopherol radicals, the reaction (b) in Fig. 4.4 will move forward, producing lipid radicals which explains the earlier oxidation process, compared to the 0.1% tocopherol treatment. As the tocopherol radicals are diminished, the equilibrium will shift so that the reactants will be favored again and the reactions will move in reverse, offering an explanation for the observation that the concentrations of 9-HODE and aldehyde in the 2% tocopherol-spiked oil increased slowly late in the experiment and were overtaken by the control group. In other words, tocopherol showed antioxidant capacity again as its concentration was reduced. The correlation between concentrations of α -tocopherol and all other oxidation products is needed for a more concrete theory of the mechanism to explain its prooxidant capacity. In this research, I was unable to quantify α -tocopherol because it eluted in both the non-polar fraction and polar fraction 1 during the SPE procedure. New SPE parameters must be optimized to allow the collection of α -tocopherol in future work.

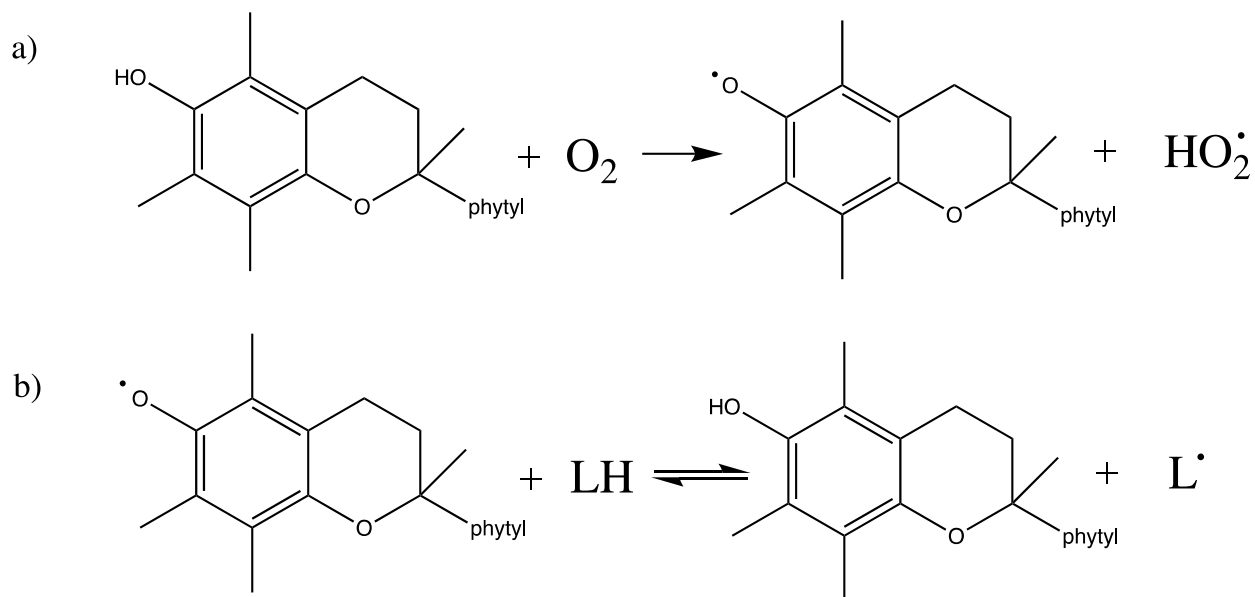


Fig. 4. 4 Mechanism of the prooxidant capacity of α -tocopherol, where L is lipid chain.

In addition to the large standard deviation, the relatively low temperature used to accelerate oxidation in this experiment is also likely a reason for the similarity between the 2% tocopherol-spiked group and the control group. Frankel (2005) alleged that the reactions in Fig. 4.4 would be dominant not only at high concentrations of antioxidants but also at elevated temperatures. Intense oxidation conditions, such as high temperature, or in the presence of catalyst or other oxidation promoters, will likely lead to a high concentration of tocopherol radicals which will result in greater prooxidant activity of tocopherol.

This research is a verification of and supplement to the current antioxidant and prooxidant theory of α -tocopherol. Compared to Martin-Rubio et al.'s (2018) work, that identified and quantified many more classes of oxidation products in soybean oil using NMR techniques, the key improvements in the experiments in this thesis was the use of pure trilinolein as substrate and GC-

MS to identify products. The soybean oil Martin-Rubio et al (2018) used contains triacylglycerols consisting of assorted fatty acids from 16:0 to 18:3n-3, which is likely to contribute to the range of products identified. Furthermore, the authors failed to note that soybean oil contains natural tocopherol which would influence the results. The adoption of trilinolein in this research would not only lead to complete identification of all oxidation products, but also remove the influence of natural tocopherol that exists in commercial oils. On the other hand, although more oxidation products were detected by NMR than using GC, GC-MS was able to provide the specific structure of each product. For instance, although Martin-Rubio et al (2018) identified and quantified total hydroxy FAME, the position of the hydroxy groups and the double bonds remained unknown. In that case, further analysis of oxidation pathways would be difficult. Moreover, their data was unable to support an antioxidant theory of α -tocopherol, showing a rapid increase in oxidation products as α -tocopherol concentration increased. They suggested that the oxidation pathways changed when α -tocopherol was present because of the earlier formation of oxidation products, but did not show data to support this. However, they did identify and quantify total hydroperoxides successfully, which was an omission in the current research. The correlation between hydroperoxides and the other secondary oxidation products is key information in determining the oxidation pathways when tocopherol is present. The failure to quantify hydroperoxides in this work may be due to their loss during the sample preparation process; the SPE procedure was originally optimized for recovery of epoxides and hydroxides and it may be that hydroperoxides were not eluted from the column with that method.

4.3.2 The Formation of Epoxides

Epoxides are known as important intermediate compounds in the decomposition reaction of hydroperoxides in oxidation pathways suggested by Hamberg and Gotthammar (1973). However, GC-MS analysis showed the absence of any acyl structures containing epoxides without also including hydroxy functionalities during the whole experimental cycle, which does not support the intermediate compound theory of epoxides. There are a number of possible reasons which could explain the absence of epoxides.

For polyunsaturated lipids, in addition to the production of hydroperoxides through the classical chain reaction, a peroxy radical could directly attack the double bond generating an epoxide and an alkoxy radical (Fig. 1.1) (Frankel, 1984; Giuffrida et al. 2004). Following this pathway, epoxides may be produced very early in the oxidation process with lipids in the absence of antioxidants. As described in 4.3.1, α -tocopherol would act as a prooxidant by accelerating the formation of hydroperoxides at high concentration. With the presence of a hydrogen-donating antioxidant in this work, HODE and hydroxy-epoxy FAME would all be produced from the decomposition of hydroperoxide, rather than the peroxy radical reacting with the double-bond (Fig. 4.2). In this way, the formation of hydroperoxides would have dominated over epoxides. Hence, the epoxy functionalities will be formed after the formation of hydroxy compounds, directly producing hydroxy-epoxy FAME. However, there were no signs of the reduction of hydroxy compounds in quantification results of samples treated by 2% tocopherol; at any time point, there were also higher concentrations of hydroxy-epoxy structures than hydroxy compounds, which indicated that the hydroxy and epoxy functionalities might be generated simultaneously during hydroperoxide decomposition. In this way, the determination of hydroperoxides as major oxidation

products and epoxy-hydroxy FAME as minor products would be an efficient means for quality evaluation of commercial vegetable oils, which often contain tocopherols.

Moreover, literature suggests that α -tocopherol may also be responsible for the inhibition of hydroperoxide decomposition (Frankel, 1994; Koskas et al., 1984). Frankel and Gardner (1989) also reported that the volatile products produced through the decomposition of hydroperoxides declined with high concentrations of tocopherol during thermal oxidation. To summarize the effects, α -tocopherol at high concentrations should accelerate the formation of hydroperoxides and also inhibit their decomposition. In other words, the formation of total secondary oxidation products, such as aldehydes, epoxides and hydroxides, would be delayed during the entire oxidation process. This switch in pathways is likely to not only contribute to the absence of epoxides, but to also lead to a lower rate of formation for oxidation products other than hydroperoxides, agreeing with the trends in my data for epoxides, hydroxides and aldehydes in 2% tocopherol-spiked oil.

Further, the specific conditions employed in the thermal oxidation process will almost certainly affect the oxidation pathways. Other work which reported the presence of epoxides and the prooxidant capacity of α -tocopherol all used oxidation temperatures over 60 °C and maximum oxidation times of more than 20 days (Xia and Budge, 2018; Martin-Rubio et al., 2018; Hopia et al., 1996; Frankel, 1989; Koskas et al., 1984). Although literature focusing on the efficiency of α -tocopherol at different temperatures was not found, thermal parameters are likely to affect the formation of epoxides and the capacity of α -tocopherol as observed in this study.

4.3.3 The Formation of Aldehydes

Aldehydes have been regarded as the terminal products of lipid oxidation in all oxidation pathways. The reactivity and toxicity of aldehydes was first confirmed in experiments with animals (Kanazawa and others, 1985). Research that followed connected aldehydes to various pathological diseases such as chronic inflammation, neurodegenerative disease, adult respiratory distress syndrome and different types of cancer (Esterbauer et al., 1991; Blair, 2001). In this research, due to the adoption of a single triacylglycerol as substrate, 9-oxo-nonanoic acid was the only type of aldehyde which was identified and quantified. Moreover, the reason why I only detected a single type of aldehyde was that short chain aldehydes produced by cleavage were likely to be evaporated during the thermal oxidation process; aldehydes bonded to the triacylglycerol backbone were likely to remain in substrate. In other words, the determination of aldehydes bonded to TAG as oxidation products was reliable for evaluating the degree of oxidation. As noted in Fig. 3.8, the concentration of the aldehyde in 2% tocopherol treated samples showed a sharp increase at day 5 (~ 2 to 10 mmol mol^{-1}), compared to the other oxidation products (~ 0 to $2.5 \text{ mmol mol}^{-1}$ for HODE and 0.5 to $4.5 \text{ mmol mol}^{-1}$ for hydroxy-epoxy FAME). As described in 4.3.2, the double-bond reaction, producing hydroxide and epoxide directly, is inhibited by the formation of hydroperoxides in high concentration tocopherol-spiked oil. The pathway in Fig. 4.2 would become more favorable. Thus, the aldehyde is very likely formed from the decomposition of HODE and hydroxy-epoxy FAME. In other words, the inhibition of pathways producing hydroxide and epoxide directly, and their subsequent decomposition when formed, lead to a much lower concentrations of all oxidation products identified here, except aldehydes. Thereby the concentration of epoxides, hydroxides and epoxy-hydroxy FAME might not be higher than the control group although α -tocopherol contributed prooxidant capacity.

CHAPTER 5 CONCLUSION

In this work, the antioxidant capacity of α -tocopherol at 0.1% and at 30 °C was successfully demonstrated. The concentration of all secondary oxidation products remained at low levels with a low oxidation rate during a 15-day experimental cycle compared to both the control group and the high concentration tocopherol group. Moreover, there was no indication that the oxidation products were likely to increase sharply in the future.

High concentrations of α -tocopherol at 2% affected not only the oxidation rate of lipids, but also the pathways of lipid oxidation. The concentration of 13-HODE was significantly higher in the 2% tocopherol group than the control group at day 10 and 15, which met the expectations of higher concentrations of alcohols because of the hydrogen-donating ability of α -tocopherol. Although I was not able to statistically demonstrate the prooxidant capacity of 2% tocopherol for the other oxidation products, earlier formation of 13-HODE and aldehyde was also obvious. Moreover, the rate of formation of 13-HODE at high concentrations of tocopherol was surprisingly lower than the control group. The formation of epoxy-hydroxy lipids and the inhibition of alternative oxidation pathways were thought to be the reasons. In other words, with high concentrations of tocopherol, hydroxy lipids would transform into epoxy-hydroxy lipids rapidly; chain autooxidation pathways would be favored, which reduces the concentrations of hydroxy lipids produced through polyunsaturated lipids alternative pathways. These, combined with the high variability in the experimental data, likely led to the failure to identify a clear prooxidant capacity of high concentrations of α -tocopherol in this research. The reduction of tocopherol to low concentrations during oxidation could also have provided some antioxidant capacity as the experiment progressed. However, that is more likely to happen in the very end of the thermal

oxidation process and the oxidation time of this experiment was unlikely to be of sufficient duration.

For future work, the identification and quantification of hydroperoxides in lipids are necessary to prove the influence of α -tocopherol at high concentrations on lipid pathways and oxidation products, such as accelerating the formation of hydroperoxides, the inhibition of their decomposition and the alternative oxidation pathways. To supplement this, the quantification of tocopherol in the substrate is also necessary to monitor the antioxidant concentration in the lipids. Last but not least, the separation of all the HODEs in chromatogram should be pursued to eliminate the peak tails.

REFERENCES

- Aruoma OI, Halliwell B, Aeschbach R, & Löliger J. (1992). Antioxidant and pro-oxidant properties of active rosemary constituents: carnosol and carnosic acid. *Xenobiotica*, 22(2), 257-268.
- American Oil Chemists' Society., & Firestone, D. (2009). Official methods and recommended practices of the AOCS (6th ed.). Urbana, Ill.: AOCS.
- Barriuso, B., Astiasarán, I., & Ansorena, D. (2012). A review of analytical methods measuring lipid oxidation status in foods: a challenging task. *European Food Research and Technology*, 236(1), 1-15. doi: 10.1007/s00217-012-1866-9
- Barros, A.I.R.N.A., Nunes, F.M., Gonçalves, B., Bennett, R.N., Silva, A.P., 2011. Effect of cooking on total vitamin C contents and antioxidant activity of sweet chestnuts (*Castanea sativa* Mill.). *Food Chem.* 128, 165–172.
- Bang HO, Dyerberg J, Nielsen AB. (1971). Plasma lipid and lipoprotein pattern in Greenlandic west-coast Eskimos. *Lancet*, 1(7701), 1143-1146.
- Bang HO, Dyerberg J, Hjøorne N. (1976). The composition of food consumed by Greenland Eskimos. *Acta Medica Scandinavica*. 200(1-2), 69-73.
- Blair, I. A. (2001). Lipid hydroperoxide-mediated DNA damage. *Exp. Geront.*, 36:1473–1481.
- Buchgraber M, Ulberth F, Emons H, Anklam E. 2004. Triacylglycerol profiling by using chromatographic techniques. *Eur J Lipid Sci Technol* 106:621–48.

Chan, H. (1987). *Autoxidation of unsaturated lipids (Food science and technology)*. London; Toronto: Academic. Jia (2015). Evidence for multiple oxidation pathways from non-volatile products of methyl linoleate. For the degree of Doctor of Philosophy.

Commission Regulation (EU) No 1129/2011 of 11 November 2011 amending Annex II to Regulation (EC) No 1333/2008 of the European Parliament and of the Council by establishing a Union list of food additives. *Official Journal of the European Union*, 12. 11.2011, L 295/1-177.

Damodaran, S., Parkin, K., & Fennema, O. R. (2008). *Fennema's food chemistry* (4th ed.). Boca Raton: CRC Press/Taylor & Francis.

Dupard-Julien, C. L., Kandlakunta, B., & Uppu, R. M. (2007). Determination of epoxides by high-performance liquid chromatography following derivatization with N, N-diethylthiocarbamate. *Analytical and Bioanalytical Chemistry*, 387(3), 1027-1032. doi: 10.1007/s00216-006-1003-3.

Erkan N, Ayranci G, Ayranci E. (2008). Antioxidant activities of rosemary (*osmarinus officinalis* l) extract, blackseed (*nigella sativa*) essential oil, carnosic acid, rosmarinic acid and sesamol. *Food Chemistry*, 110(1), 76-82.

Esterbauer, H., Schaur, R. J., and Zollner, H. (1991). Chemistry and biochemistry of 4-hydroxy-2-nonenal, malonaldehyde and related aldehydes. *Free Radical Biol. Med.*, 11:81–128.

Firestone D. 2009. *Official methods and recommended practices of the AOCS*. 6th ed. Urbana: American Oil Chemists' Society Press.

- Frankel, E. N., Cooney, P.M., Moser, H.A., Cowan, J.C. and Evans, C.D. (1959a). Effect of antioxidants and metal inactivators in tocopherol-free soybean oil. *Fette Seifen, Anstrichm.* 10, 1036-1039.
- Frankel, E. N. (1984). Chemistry of free radical and singlet oxidation of lipids. *Progress in Lipid Research*, 23(4), 197-221. doi: 10.1016/0163-7827(84)90011-0
- Frankel, E. N. (1987). Secondary products of lipid oxidation. *Chemistry and Physics of Lipids*, 44(2-4), 73-85. doi: 10.1016/0009-3084(87)90045-4
- Frankel, E., & Gardner, H. (1989). Effect of alpha-tocopherol on the volatile thermal decomposition products of methyl linoleate hydroperoxides. *Lipids*, 24(7), 603-8.
- Frankel EN. (2005). Introduction. In *Lipid oxidation (second edition)* (pp. 1-14). Bridgewater: The Oily Press.
- Frankel EN. (2005). Chapter 1: Free Radical Oxidation. In *Lipid oxidation (second edition)* (pp. 15-24). Bridgewater: The Oily Press.
- Frankel EN. (2005). Chapter 9: Antioxidants. In *Lipid oxidation (second edition)* (pp. 209-258). Bridgewater: The Oily Press.
- Fruebis J, Parthasarathy S, and Steinberg D. Evidence for a concerted reaction between lipid hydroperoxides and polypeptides. *Proc Natl Acad Sci U S A* 89: 10588–10592, 1992.
- Fukumoto, L., & Mazza, G. (2000). Assessing antioxidant and prooxidant activities of phenolic compounds. *Journal of Agricultural and Food Chemistry*, 48(8), 3597-604.

- Gardner, H.W., Kleiman, R., & Weisleder, D. (1974). Homolytic decomposition of linoleic acid hydroperoxide: Identification of fatty acid products. *Lipids*, Sept(9), 696-706.
- G´erard HC, Moreau RA, Fett WF, Osman SF. 1992. Separation and quantitation of hydroxy and epoxy fatty acid by high-performance liquid chromatography with an evaporative light-scattering detector. *J Am Oil Chem Soc* 69:301–4.
- Goicoechea E, Guill´en MD. 2010. Analysis of hydroperoxides, aldehydes and epoxides by ¹H nuclear magnetic resonance in sunflower oil oxidized at 70 and 100°C. *J Agric Food Chem* 58:6234–45.
- Grüneis, V., Fruehwirth, S., Zehl, M., Ortner, J., Schamann, A., König, J., & Pignitter, M. (2019). Simultaneous analysis of epoxidized and hydroperoxidized triacylglycerols in canola oil and margarine by LC-MS. *Journal of Agricultural and Food Chemistry*, 67(36), 10174-10184.
- Giuffrida, F., Destailats, F., Robert, F., Skibsted, L. H., & Dionisi, F. (2004). Formation and hydrolysis of triacylglycerol and sterols epoxides: role of unsaturated triacylglycerol peroxy radicals. *Free Radical Biology and Medicine*, 37(1), 104-114. doi: 10.1016/j.freeradbiomed.2004.04.004
- Goicoechea, E. n., & Guillen, M. a. D. (2010). Analysis of hydroperoxides, aldehydes and epoxides by ¹H nuclear magnetic resonance in sunflower oil oxidized at 70 and 100 °C. *Journal of Agricultural and Food Chemistry*, 58(10), 6234-6245. doi: 10.1021/jf1005337

- Gordon, M. H. The mechanism of antioxidant action in vitro. In Food Antioxidants; Hudson, B. J. F., Ed.; Elsevier Applied Science: London, U.K., 1990; pp 1-18.
- Guill'en MD, Uriarte PS. 2012a. Monitoring by ¹H nuclear magnetic resonance of the changes in the composition of virgin linseed oil heated at frying temperature. Comparison with the evolution of other edible oils. Food Control 28:59–68.
- Gunstone, F. D., Harwood, J. L., & Dijkstra, A. J. (2007). The lipid handbook with CD-ROM (3rd ed.). Boca Raton: CRC Press.
- Kanazawa, K., Kanazawa, E., and Natake, M. (1985). Uptake of secondary autoxidation products of linoleic acid by the rat. Lipids, 20:412–419.
- Knothe G, Kenar JA. 2004. Determination of the fatty acid profile by ¹H-NMR spectroscopy. Eur J Lipid Sci Technol 106:88–96.
- Koskas, J. P., Cillard, J., & Cillard, P. (1984). Autoxidation of linoleic acid and behavior of its hydroperoxides with and without tocopherols. Journal of the American Oil Chemists' Society, 61, 1466–1469.
- Kulås, E., Olsen, E., & Ackman, R. (2002). Effect of α -, γ -, and δ -tocopherol on the distribution of volatile secondary oxidation products in fish oil. European Journal of Lipid Science and Technology, 104(8), 520-529.
- Haberland ME, Olch CL, and Fogelman AM. Role of lysines in mediating interaction of modified low-density lipoproteins with the scavenger receptor of human monocyte macrophages. J Biol Chem 259: 11305–11311, 1984.

- Hamberg, M., & Gotthammar, B. (1973). A new reaction of unsaturated fatty acid hydroperoxides: Formation of 11-hydroxy-12,13-epoxy-9-octadecenoic acid from 13-hydroperoxy-9,11-octadecadienoic acid. *Lipids*, 8(12), 737-744.
- Hopia, A., Huang, S., & Frankel, E. (1996). Effect of α -tocopherol and Trolox on the decomposition of methyl linoleate hydroperoxides. *Lipids*, 31(4), 357-365.
- Ingold KU. (1961). Inhibition of the autoxidation of organic substances in the liquid phase. *Chemical Reviews*, 61(6), 563-589.
- Jurgens G, Lang J, and Esterbauer H. Modification of human low density lipoproteins by the lipid peroxidation product 4-hydroxynonenal. *Biochim Biophys Acta* 875: 103–114, 1986.
- Lambert, J. B. (1987). *Introduction to organic spectroscopy*. New York: Macmillan.
- Lampi, A.-M., Kataja, L., Kamal-Eldin, A., & Vieno, P. (1999). Antioxidant activities of α - and γ -tocopherols in the oxidation of rapeseed oil triacylglycerols. *Journal of the American Oil Chemists' Society*, 76, 749–755.
- Marmesat, S., Velasco, J., & Dobarganes, M. C. (2008). Quantitative determination of epoxy acids, keto acids and hydroxy acids formed in fats and oils at frying temperatures. *Journal of Chromatography A*, 1211(1-2), 129-134. doi: 10.1016/j.chroma.2008.09.077

- Martínez-Yusta, A., & Guillén, M. D. (2014). Deep-frying food in extra virgin olive oil: A study by ¹H nuclear magnetic resonance of the influence of food nature on the evolving composition of the frying medium. *Food Chemistry*, 150, 429-437.
doi:10.1016/j.foodchem.2013.11.015
- Martin-Rubio, A., Sopelana, P., Ibargoitia, M., & Guillén, M. (2018). Prooxidant effect of α -tocopherol on soybean oil. Global monitoring of its oxidation process under accelerated storage conditions by ¹H nuclear magnetic resonance. *Food Chemistry*, 245, 312-323.
- Marai L, Myher JJ, Kuksis A. 1983. Analysis of triacylglycerols by reversed-phase high pressure liquid chromatography with direct liquid inlet mass spectrometry. *Can J Biochem Cell Biol* 61:840–9.
- Mäkinen, E. M., & Hopia, A. I. (2000). Effects of α -tocopherol and ascorbyl palmitate on the isomerization and decomposition of methyl linoleate hydroperoxides. *Lipids*, 35, 1215–1223.
- McClements, D.J. & Decker, E.A. (2008). Chapter 4: Lipids. In S. Damodaran, K.L. Parkin & O.R. Fennema (Eds.), *Fennema's Food Chemistry* (4th ed.). CRC Press.
- McGEE, H., *Fats, in on Food and cooking - The Science And Lore Of The Kitchen*. 2004, Scribner: New York, NY.
- Mozaffarian, D., Katan, M., Ascherio, A., Stampfer, M., & Willett, W. (2006). Trans fatty acids and cardiovascular disease. *The New England Journal of Medicine*, 354(15), 1601-1613.

- Morales, A., Marmesat, S., Dobarganes, M. C., Márquez-Ruiz, G., & Velasco, J. (2012). Quantitative analysis of hydroperoxy-, keto- and hydroxy-dienes in refined vegetable oils. *Journal of Chromatography A*, 1229, 190-197. doi: 10.1016/j.chroma.2012.01.039
- Mubiru, E., Shrestha, K., Papastergiadis, A., & De Meulenaer, B. (2013). Improved gas chromatography-flame ionization detector analytical method for the analysis of epoxy fatty acids. *Journal of Chromatography A*, 1318, 217–225.
- Raghavamenon, A., Garelnabi, M., Babu, S., Aldrich, A., Litvinov, D., & Parthasarathy, S. (2009). Alpha-tocopherol is ineffective in preventing the decomposition of preformed lipid peroxides and may promote the accumulation of toxic aldehydes: A potential explanation for the failure of antioxidants to affect human atherosclerosis. *Antioxidants & Redox Signaling*, 11(6), 1237-1248.
- Repetto, M., Semprine, J., & Boveris, A. (2012). Lipid peroxidation: chemical mechanism, biological implications and analytical determination. doi: 10.5772/45943
- Richheimer SL, Bernart MW, King GA, Kent MC, Beiley DT. (1996). Antioxidant activity of lipid-soluble phenolic diterpenes from rosemary. *Journal of the American Oil Chemists' Society*, 73(4), 507-514.
- Romero, N., Robert, P., Masson, L., Ortiz, J., Pavez, J., Garrido, C., . . . Dobarganes, C. (2004). Effect of α -tocopherol and α -tocotrienol on the performance of Chilean hazelnut oil (Gevuina avellana Mol) at high temperature. *Journal of the Science of Food and Agriculture*, 84, 943-948.

- Pokorný J. (2003b). Natural antioxidant functionality during food processing. In J. Pokorný, N. Yanishlieva and M. Gordon (Eds.), *Antioxidants in Food* (pp. 331-354). Boca Raton: CRC Press.
- Poole CF. 2013. Alkylsilyl derivatives for gas chromatography. *J Chromatogr A* 1296:2–14.
- Schaich, K. M. (2005). Lipid oxidation: theoretical aspects. *Bailey's industrial oil and fat products*. doi: 10.1002/047167849X.bio067
- Schaich, K. M. (2012). Thinking outside the classical chain reaction box of lipid oxidation. *Lipid Technology*, 24(3), 55–58. <https://doi.org/10.1002/lite.201200170>
- Simopoulos AP. (1991). Omega-3 fatty acids in health and disease and in growth and development. *The American Journal of Clinical Nutrition*, 54(3), 438-463.
- Taghvaei, M., & Jafari, S. M. (2015). Application and stability of natural antioxidants in edible oils in order to substitute synthetic additives. *Journal of Food Science and Technology*. <https://doi.org/10.1007/s13197-013-1080-1>
- Thompson, M.; Ellison, S. L. R.; Wood, R. (2002). Harmonized guidelines for single-laboratory validation of methods of analysis (IUPAC Technical Report). *Pure and Applied Chemistry*, 74(5), 835-855.
- Valko M, Leibfritz D, Moncol J, Cronin MTD, Mazur M, Telser J. (2007). Free radicals and antioxidants in normal physiological functions and human disease. *International Journal of Biochemistry & Cell Biology*, 39(1), 44-84.

- Villanueva, C., Kross, R.D., 2012. Antioxidant-induced stress. *Int. J. Mol. Sci.* 13, 2091–2109.
- Wagner, K. H., & Elmadfa, I. (2000). Effects of tocopherols and their mixtures on the oxidative stability of olive oil and linseed oil under heating. *European Journal of Lipid Science and Technology*, 102, 624–629.
- Weber, N. (1997). Deep frying. Chemistry, nutrition, and practical applications. Edited by E. G. Perkins, and M. D. Erickson. V and 357 pages, numerous figures and tables. AOCS Press, Champaign, Illinois, 1996. Price: 60.00 US \$. *Food / Nahrung*, 41(4), 247.
- Weihrauch JL, Brewington CR, Schwartz DP. 1974. Trace constituents in milk fat: isolation and identification of oxofatty acids. *Lipids* 9:883–90.
- Wilson R, Smith R, Wilson P, Shepherd MJ, Riemersma RA. 1997. Quantitative gas chromatography-mass spectrometry isomer-specific measurement of hydroxy fatty acids in biological samples and food as a marker of lipid peroxidation. *Anal Biochem* 248:76–85.
- Xia, W., & Budge, S. M. (2017). Techniques for the analysis of minor lipid oxidation products derived from triacylglycerols: epoxides, alcohols, and ketones. *Comprehensive Reviews in Food Science and Food Safety*, 16(4), 735–758. <https://doi.org/10.1111/1541-4337.12276>
- Xia, W., & Budge, S. M. (2017). GC-MS characterization of hydroxy fatty acids generated from lipid oxidation in vegetable oils. *European Journal of Lipid Science and Technology*, 1700313, 1700313. <https://doi.org/10.1002/ejlt.201700313>

Xia, & Budge. (2018). Simultaneous quantification of epoxy and hydroxy fatty acids as oxidation products of triacylglycerols in edible oils. *Journal of Chromatography A*, 1537, 83-90.